
Retrospective Theses and Dissertations

Summer 1980

A Parametric Study of Economical Energy Usage in Freeze Tunnels

Marc A. Harrison
University of Central Florida



Part of the [Engineering Commons](#)

Find similar works at: <https://stars.library.ucf.edu/rtd>

University of Central Florida Libraries <http://library.ucf.edu>

This Masters Thesis (Open Access) is brought to you for free and open access by STARS. It has been accepted for inclusion in Retrospective Theses and Dissertations by an authorized administrator of STARS. For more information, please contact STARS@ucf.edu.

STARS Citation

Harrison, Marc A., "A Parametric Study of Economical Energy Usage in Freeze Tunnels" (1980).
Retrospective Theses and Dissertations. 491.
<https://stars.library.ucf.edu/rtd/491>



A PARAMETRIC STUDY
OF ECONOMICAL ENERGY
USAGE IN FREEZE TUNNELS

BY

MARC A. HARRISON
B.S., United States Naval Academy, 1973

THESIS

Submitted in partial fulfillment of the requirements
for the degree of Master of Science
in the Graduate Studies
Program of the College of Engineering
at the University of Central Florida;
Orlando, Florida

Summer Quarter
1980

ABSTRACT

An investigation into economical energy usage in freeze tunnels was conducted. Freeze tunnels are commonly used in the food processing industry to freeze products, and in some cases may use large amounts of electricity. An actual freeze tunnel was observed and modeled on a computer.

A parameter study was conducted. The results of the parameter study indicate the efficiency and energy costs in freeze tunnels may vary widely. Important parameters included the Nusselt number, air temperature, and the ratio of fan work divided by the useful refrigeration effect. Although no single set of optimum conditions were found, methods for improving the effectiveness of freeze tunnels, both in existing and future designs, were discussed. It was also concluded that the ratio of fan work to the freeze tunnel's useful refrigeration effect was a dominant factor in the energy cost of operating a freeze tunnel.

ACKNOWLEDGEMENTS

The author would like to sincerely thank all those who helped provide the wide variety of technical advice, information, and support necessary to complete this investigation. Thanks to Dr. D. Linton, Dr. E. R. Hosler and Professor J. Beck who provided invaluable technical advice. Also to Dr. B. Eno who provided departmental support in obtaining the necessary equipment to complete the study. Thanks to the owners and operators of the citrus cooperative who were helpful and allowed their tunnel to be observed. Thanks to Mrs. Linda Stewart, who typed the report and to Mrs. Black, the bibliographer for her help and advice. Special thanks to Dr. P. J. Bishop who advised and provided help, guidance, and support through every phase of this investigation.

This investigation was partially funded by a State of Florida research grant through the Engineering and Industrial Experiment Station at the University of Central Florida.

TABLE OF CONTENTS

	Page
ACKNOWLEDGEMENTS	iii
Chapter	
I. INTRODUCTION	1
Introduction	
Freeze Tunnel Description	
II. THEORY	5
The Freeze Tunnel Coefficient of Performance	
The Heat Removal Rate From Cylindrical Cans of Citrus Concentrate	
Convective Heat Transfer Coefficient	
Model	
III. MEASUREMENTS	20
Measurements	
Production Rate	
Air Flow Rate	
Temperatures	
Average Nusselt Number	
Implications of the Measurements on the Parameter Study	
IV. THE PARAMETER STUDY	43
The Coefficient of Performance of the Freeze Tunnel	
Variation in the Coefficient of Performance of the Refrigeration Plant with Freeze Tunnel Air Temperature	
Variation in the Fan Work with Nusselt Number	
The Freeze Tunnel Coefficient of Performance Versus the Nusselt Number	

The Freeze Tunnel Coefficient of
Performance Versus Freeze Tunnel Capacity
Energy Costs Versus Freeze Tunnel
Capacity
Results Concerning the Observed
Freeze Tunnel
Results for Freeze Tunnel Design
in General

V. CONCLUSIONS	63
Limitations of Study	
Significant Results	
Possibilities for Further Research	
APPENDIX	67
BIBLIOGRAPHY	73

TABLES

	Page
1 - Effective Thermal Properties for Brix° 44.8 Citrus Concentrate	11
2 - Summary of Freeze Tunnel Characteristics	39
3 - Summary of Cooling Loads	41
4 - Coefficient of Performance of the Refrigeration Unit	48

ILLUSTRATIONS

	Page
1 - Freeze Tunnel Sketch	3
2 - Volume Element and Nodal Arrangement	17
3 - Freeze Tunnel Air Flow Sketch	22
4 - Top View of Observed Packing Arrangement	25
5 - Temperature Data	29
6 - Average Temperature of Concentrate vs. Time	31
7 - Comparison of Measured and Computer Predicted Values of the Average Temperature of Concentrate versus Time in the Freeze Tunnel	36
8 - Freeze Tunnel Coefficient of Performance, Divided by the Refrigeration Unit Coefficient of Performance vs. Fan Power Divided by the Useful Refrigeration Effect	45
9 - Freeze Tunnel Coefficient of Performance vs. Refrigeration Unit Coefficient of Performance	46
10 - Freeze Tunnel Coefficient of Performance, Divided by the Refrigeration Unit Coefficient of Performance vs. the Nusselt Number	51
11 - Freeze Tunnel Coefficient of Performance vs. the Nusselt Number	52
12 - Freeze Tunnel Coefficient of Performance vs. Freeze Tunnel Capacity	54
13 - Freeze Tunnel Electricity Cost vs. Freeze Tunnel Capacity	57
14 - Freeze Tunnel Electricity Cost Per Unit Processed vs. Freeze Tunnel Capacity	58

CHAPTER 1
INTRODUCTION

1.1 INTRODUCTION

An investigation into economical energy usage in freeze tunnels was conducted. The primary objective of this investigation, was to determine the effects of the important design and operating parameters on energy consumption in these devices. Freeze tunnels are commonly used in the food processing industry to rapidly freeze or reduce the temperature of food products. Rapid cooling is often required to preserve food quality and to meet production goals. In some cases, the cost of operation of freeze tunnels is a small part of the cost of the entire food processing operation [1]. But, as energy costs continue to rise efficient energy usage will become more important. In other cases energy consumption in freeze tunnels is already a large part of the energy consumed in the entire operation. One study estimated for a medium sized citrus juice concentrate processing plant, about 25% of the total energy costs, of about 1.4×10^6 dollars per season, was due to freeze tunnel electricity consumption [2].

The parameter study was accomplished with a computer model of a freeze tunnel. The computer model was based on an actual freeze tunnel that was available for observation. Measurements of the actual freeze tunnel's typical operating conditions were made and compared with predictions of the computer model. The computer model was initially pro-

grammed to simulate actual tunnel operating conditions as closely as possible. After the validity of the model was demonstrated, important parameters were varied from the actual conditions measured for the observed tunnel. The effects of the parameter variations on the freeze tunnel's effectiveness was then evaluated.

1.2 FREEZE TUNNEL DESCRIPTION

Freeze tunnel designs may vary with usage, capacity, food product, and manufacturer. The tunnels studied in this report are used to rapidly reduce the temperature of orange and grapefruit juice concentrate just after it is canned. Parameters that affect energy consumption in the tunnel observed are assumed to have similar effects in freeze tunnels in general. In any freeze tunnel, energy is consumed primarily by the fans and the refrigeration units. Figure 1 is a simple sketch of the freeze tunnel observed with approximate dimensions.

The freeze tunnel is used by a citrus concentrate plant in Central Florida. It is located inside a large building which shields it from environmental extremes. Right circular cylindrical cans of citrus concentrate enter the freeze tunnel on a mesh conveyor belt. In general, the cans stand upright and are packed tightly together. Refrigerated air is blown between the cans by large fans to maintain a high rate of heat transfer and short freezing times. Although, the conveyor belt is driven by a single speed motor and reduction gear, the conveyor belt may be stopped for short periods of time as required by events in other parts of the production line. Ideally, the cans exit the tunnel, on the conveyor belt, simultaneously with the desired freezing time. The

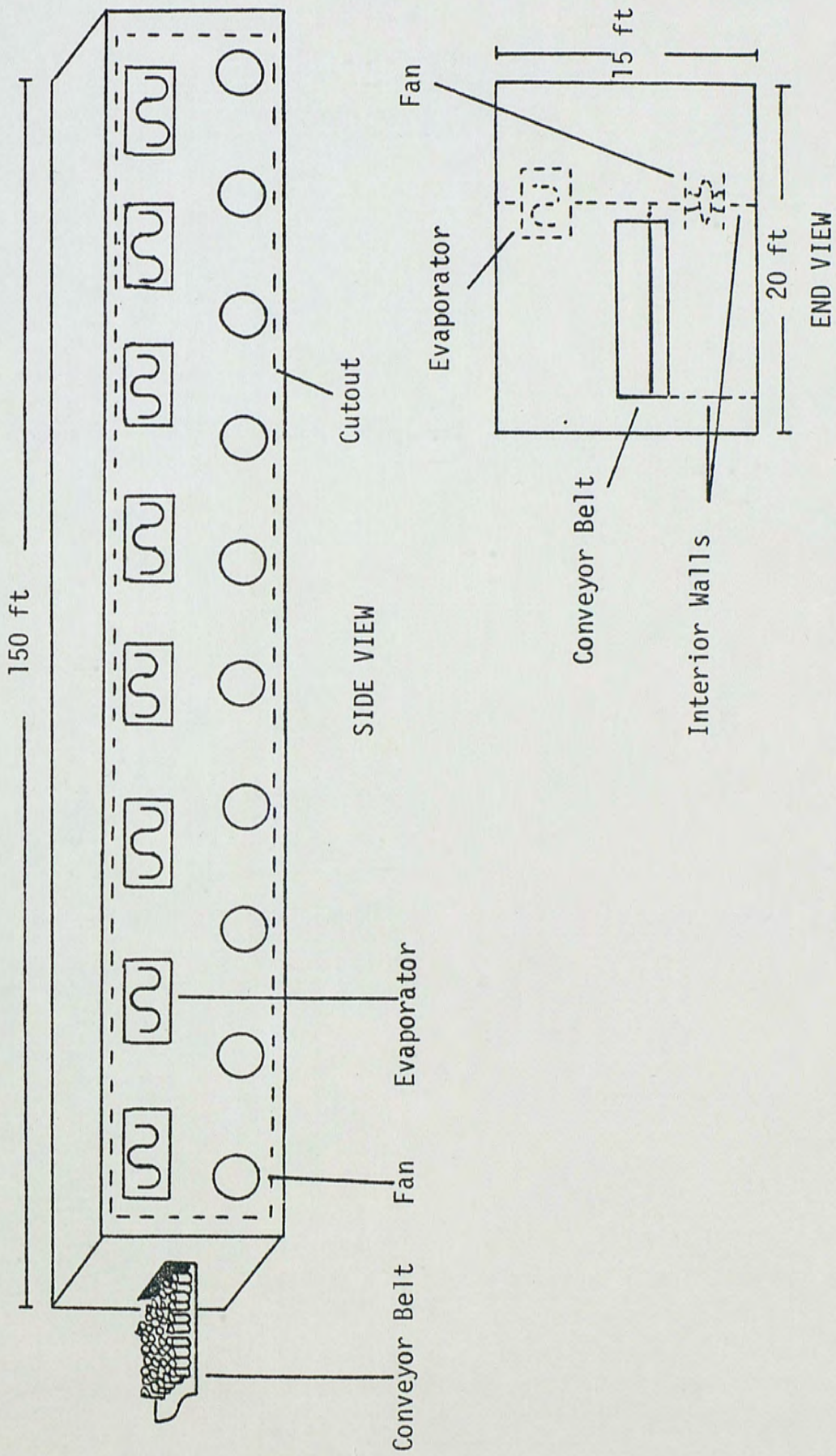


Fig. 1. Freeze Tunnel Sketch

tunnel's evaporators are supplied with ammonia refrigerant by a large two-stage, vapor compression plant. There are two large doors on opposite sides of the freeze tunnel. The ceiling and walls are insulated by 6 inches of polyurethane insulation, encased in metal. The floor is a cement slab. The quantity and type of any insulation in the floor could not be determined. The tunnel contained 10 fans rated at 10 horsepower each and 8 evaporators.

CHAPTER 2

THEORY

2.1 THE FREEZE TUNNEL COEFFICIENT OF PERFORMANCE

In this report, the coefficient of performance (COP) for the freeze tunnel is used to estimate the effectiveness of the tunnel. The coefficient of performance is defined [3] as

$$\text{COP} = \frac{\text{refrigeration effect}}{\text{net work input}}$$

In this case the useful refrigeration effect is the rate of heat removal from the concentrate, q_c . The net work input is the sum of the work of the fans, W_f , and the work of the compressors, W_c . Thus, the coefficient of performance for the tunnel COP_t , becomes

$$\text{COP}_t = \frac{q_c}{W_c + W_f} \quad (1)$$

The value of q_c is obtained by calculating the rate of change of concentrate enthalpy in the tunnel and is discussed further in the next two sections. The value of W_f is estimated from the fan ratings. The value of W_c , in this case, must be determined indirectly because the refrigeration plant supplies several loads besides the freeze tunnel. Therefore, W_c is estimated by using an energy balance to calculate the refrigeration load.

An energy balance is performed as follows. Steady state operation is assumed so the time rate of change of the stored energy equals zero. The concentrate packing material is ignored. The energy balance then becomes

$$q_1 = q_c + q_{\text{trans}} + q_{\text{inf}} + q_f \quad (2)$$

where

q_L = total refrigeration load

q_C = net rate of energy removal from concentrate

q_{trans} = transmission heat gain due to conduction and convection to the environment

q_f = rate of energy addition due to fans

Transmission heat gains are calculated with the following equation [4].

$$q_{trans} = UA (T_o - T_i)$$

where

U = air to air heat transfer coefficient

A = area of exposed surface

T_o = outside air temperature

T_i = average air temperature in refrigerated space

The value of U for the roof and walls is based on the construction [4]. The value of U for the cement slab floor is assumed to be 0.1 Btu/hr ft²F [5]. A ground temperature of 60°F is assumed. The value of T_o is based on the summer design dry bulb temperature for Central Florida for the roof and walls. The ambient temperatures were chosen as worst case values to be conservative. Values for T_i and area were either measured or chosen to correspond to expected operating conditions.

Infiltration heat gains are calculated from [4].

$$q_{inf} = 4.5 (\text{cfm}) \Delta h$$

where

cfm = cubic feet per minute of air infiltrating the tunnel

Δh = difference in enthalpy between the outside and inside air.

The change in enthalpy was calculated for design summer conditions. The cfm was calculated in two parts: the first part was the cfm due to door openings, and the second part was the cfm infiltrating with the conveyor belt. The cfm due to door openings was calculated using the procedures in ASHRAE [4]. Air is assumed to infiltrate at an average velocity of 75 ft/min. The average cfm is then calculated from the size of the door opening and the fraction of each hour the door is actually open. The second part, air that infiltrates with the food product, is calculated by assuming all air between the cans on the conveyor belt, in the void space, is removed with the cans and replaced by outside air. The volume of the void space and its volumetric flow rate can be measured or specified by operating conditions.

Finally, since the fans are entirely enclosed in the freeze tunnel, their heat addition, in BTU per hour, is given by [4].

$$q = 2995 H_p$$

where

$$H_p = \text{motor horsepower}$$

Once the refrigeration load, q_L , is determined, the required compressor work can be determined from the COP of the refrigerating plant.

$$W_c = q_L / \text{COP} \quad (3)$$

Combining equations (1) and (3) results in

$$\text{COP}_t = \frac{q_c}{(q_L / \text{COP} + W_f)} \quad (4)$$

2.2 THE HEAT REMOVAL RATE FROM CYLINDRICAL CANS OF CITRUS CONCENTRATE

In the case of a freeze tunnel, the useful refrigeration effect is the heat removal rate from the citrus concentrate in the freeze tunnel control volume, q_c , when the packing material is ignored. Calculation of q_c is complicated by the freezing process of citrus concentrate, the convective boundary condition of the can surfaces, and the substantial temperature gradients that exist in the cans and the tunnel as a result of the rapid freezing process. The best available thermal property data for citrus products has been recently compiled by Chen [6], and this data is currently being evaluated and improved by the Florida Department of Citrus.

A detailed knowledge of the temperature distribution in each can of concentrate versus time is required to mathematically model a freeze tunnel. Knowledge of the temperature distribution is necessary to determine the heat content of each can. Also, the surface temperature of each can is necessary to determine the rate of convective heat transfer from each can to the freeze tunnel environment.

Methods exist to predict temperature distribution changes in freezing problems in general [7,8,9]. Common methods involve assuming a boundary exists between regions of frozen and unfrozen liquids. Each region has appropriate thermal properties and the latent heat is assumed to be evolved at the boundary as it moves through the freezing material. However, as pointed out by Keller and Ballard [9], the freezing process in fruit juice is different.

They considered fruit juice solutions to have the freezing properties of a typical two phase system of ice and solution. In equilibrium, at a given temperature below the freezing point, a given amount of ice exists with a given amount of solution at a certain concentration. Any change in equilibrium temperature alters the amount of ice and solution with a corresponding change in the solution concentration. As the amount of ice and solution changes with temperature, the thermal properties change. Also, the latent heat of fusion for the ice is released or generated over a range of temperatures.

Keller and Ballard calculated values of effective thermal properties over a range of temperatures and citrus juice concentrations. The effective thermal properties, specifically the effective specific heat capacity, c_{ef} , effective thermal conductivity, k_{ef} , and density, ρ , include the effects of the latent heat of fusion and any thermal property changes with temperature [9].

Effective thermal property data are used in this investigation. The data chosen correspond to a citrus juice concentration at Brix^o 44.8 which is currently a legal standard for Florida orange juice concentrate. Unfortunately, effective thermal property data of concentrate are only available down to temperatures of -20°F and the freeze tunnels considered have been observed producing air temperatures down to about -40°F. Therefore, it was assumed the thermal property data were constant between -20°F and -40°F. The properties are relatively constant with temperature near -20°F. Also temperatures below -20°F were very rarely predicted by the computer and never observed. A summary of the actual data used is listed in

table 1

Once the effective specific heat capacity, c_{ef} , is known, the heat removal rate from the concentrate can be estimated by integrating

$$q_c = \dot{m} \int c_{ef} dT \quad (5)$$

where

\dot{m} = concentrate mass flow rate through the freeze tunnel

T = concentrate temperature

The integrations were accomplished graphically between the average concentrate temperatures at the tunnel entrance and exit. Of course, this method requires established values of both average entrance and exit temperatures.

Another common method, that can be used to calculate q_c is to use Newton's law of cooling.

$$q_c = hA (T_s - T_a) \quad (6)$$

where

h = convective heat transfer coefficient

A = exposed surface area

T_s = surface temperature

T_a = air temperature

This is discussed further in Section 2.3.

TABLE 1

EFFECTIVE THERMAL PROPERTIES FOR BRIX° 44.8 CITRUS CONCENTRATE

Temperature (°F)	Specific Heat Capacity (BTU/lbm°F)	Thermal Conductivity (BTU/hr ft°F)	Density (lbm/ft ³)
16	0.73	0.18	75.2
15	5.13	2.00	75.1
10	3.86	0.72	74.3
5	2.81	0.36	73.6
0	2.00	0.35	73.0
-5	1.41	0.35	72.6
-10	1.06	0.47	72.2
-15	0.94	0.60	72.0
-20	1.00	0.65	71.7

2.3 CONVECTIVE HEAT TRANSFER COEFFICIENT

It is necessary to evaluate the convective heat transfer coefficient, h , to determine the rate of heat transfer from the citrus juice concentrate as a function of time and position in the freeze tunnel.

Whitaker [10] presented a method to calculate h for flow in packed beds. The packed bed analogy seems appropriate based on observations of the operating tunnel. Although most cans stood upright and were packed tightly, empty gaps and a few cans on their sides were scattered between regions of tightly packed cans.

The method described by Whitaker [10] is briefly presented here. The convective heat transfer coefficient, h , is defined by

$$q = h a_v V \Delta T_{ln} \quad (7)$$

where

q = total rate of heat transfer from the packing

a_v = packing surface area per unit volume

V = total volume of the packed bed

ΔT_{ln} = log mean temperature difference

The surface area per unit volume, a_v , is related to the void fraction of the bed, ϵ , which is defined as

$$\epsilon = \frac{\text{void volume in the bed}}{\text{total volume of the bed}}$$

The equation is

$$a_v = (A_p/V_p)(1-\epsilon)$$

where

A_p = particle area

V_p = particle volume

Whitaker [10] showed that the hydraulic radius of the packed bed, R_h , is given by

$$R_h = \epsilon/a_v$$

However, the characteristic length of the packed bed, L^* , was defined as

$$L^* = 6.0 R_h$$

The characteristic velocity, u^* , or the average air velocity in the bed, is defined by

$$u^* = \frac{1}{A_{\text{void}}} \int u dA_{\text{void}} \quad (9)$$

where

A_{void} = cross-sectional void area

u = local air velocity

If the bed is uniform, then

$$u^* = Q/(\epsilon A) \quad (10)$$

where

Q = air volumetric flow rate through the packed bed

A = cross-sectional area of bed

The Reynolds number, Re , the Nusselt number, Nu , and the convective heat transfer coefficient, h , are given by

$$Re = \frac{u^* L^*}{\nu}$$

$$Nu = (0.5 Re^{1/2} + 0.2 Re^{2/3}) Pr^{1/3}$$

$$h = \frac{Nu k}{L^*}$$

where

ν = kinematic viscosity of air

Pr = Prandtl number of air

k = thermal conductivity of air

2.4 MODEL

The temperature distribution in each can of concentrate must be determined to calculate the can's average temperature, heat content, and surface temperature. The temperature distribution, as a function of time and position in the tunnel, was numerically calculated using an IBM 360.

In this case, the applicable energy equation for heat flow in a cylinder with a convective boundary condition is [11].

$$\nabla^2 T = \frac{1}{\alpha} \frac{\partial T}{\partial t}$$

where

T = temperature

α = thermal diffusivity

t = time

with boundary conditions such that

$$\begin{aligned} 1) T \Big|_{t=0} &= T_i \\ 2) k \nabla T \Big|_{\text{surface}} &= h(T_s - T_\infty) \end{aligned}$$

where

T_i = initial average concentrate temperature

k = concentrate thermal conductivity

T_s = can surface temperature

T_∞ = air temperature

An analytical solution to this system is prevented by the convective boundary condition.

The numerical solution employed an implicit technique using finite differences. In this case the governing difference equations were [11]

$$\sum_j \frac{T_j^P - T_i^P}{R_{ij}} = C_i \frac{T_i^{P+1} - T_i^P}{\Delta t} \quad (11)$$

where

T^P = nodal temperature at time level P

i = nodal location

j = refers to each adjacent node

C_i = lumped system heat capacitance for node i

R_{ij} = thermal resistance between nodes i and j

Δt = time step

The resistances and capacitances are calculated by

$$C_i = \rho c \Delta V_i$$

$$R_{ij} = \frac{\Delta X_{ij}}{kA} \text{ for conduction}$$

$$R = \frac{1}{hA} \text{ for convection}$$

where

ρ = density

c - specific heat capacity

ΔV_i = volume of ith element

ΔX_{ij} = distance between nodes i and j

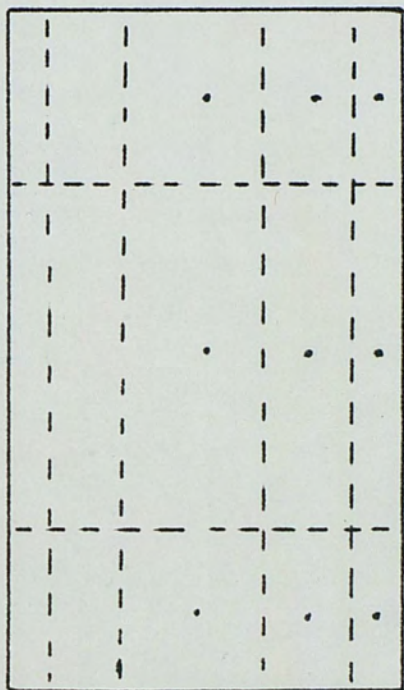
A = nodal area for heat transfer

Since an implicit method was used, the time step had to be chosen to meet adequate stability criteria. Discontinuities in the effective thermal properties around the initial freezing point required a small time step to assure a stable solution. A time step of 3.6 seconds was chosen for the 12 ounce can size.

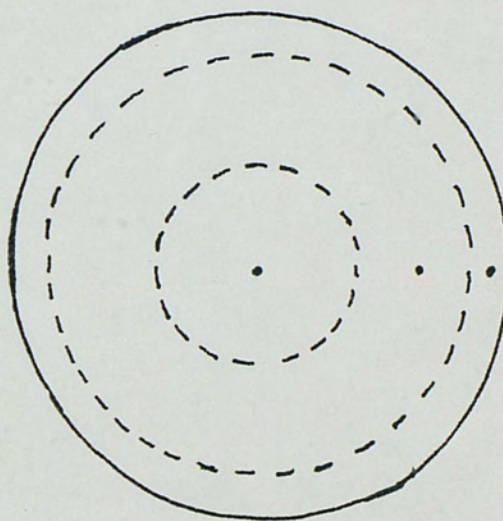
Each cylinder of concentrate was divided into 3 sets of 3 concentrate rings for a total of 9 volume elements and nodes. Various volume element arrangements were considered. The arrangement used is sketched in figure 2. The width of the outermost elements, in either the axial or radial direction, is half that of the inner elements. This arrangement improved the stability of the solution over the case where nodes are spaced equally. Also, the outer elements are thinner and provide a closer approximation of the surface temperature.

In actual concentrate cans, a small air gap exists at the top of the can. The air gap tends to insulate the top surface of the concentrate. The size of this air gap was measured, and its thermal resistance was calculated. Since the air gap's thermal resistance is in series with the convective thermal resistance of the top surface, they were summed and used as an effective convective thermal resistance for the top surface.

An additional concern was that the air temperature changes as the air flows between the concentrate cans. This effect was accounted for by using equation (7) to calculate the heat transferred to the air, q_{air} . The temperature rise of the air, can be calculated from the definition of specific heat capacity and is given by



Side view with can upright



End view

Fig. 2. Volume Element and Nodal Arrangement

$$\Delta T_a = q_{\text{air}} / (c_p \dot{m})$$

where

ΔT_a = temperature rise of the air

c_p = air specific heat capacity

\dot{m} = mass flow rate of air

Substituting equation (7) for q_{air} results in

$$\Delta T_a = (h a'_v V \Delta T_{1n}) / (c_p \dot{m}) \quad (12)$$

A value for the can's surface temperature T_s , is required for ΔT_{1n} .

The value of T_s was assumed to be uniform over each can's surface.

The computer program estimated T_s by averaging the temperature of the outer elements, weighted relative to their surface areas, at each time step. The air temperature near the surface of each volume element, for use in equation (11), was then estimated by assuming the air temperature for the surfaces of the upstream volume elements was equal to the initial air temperature. The air temperature near the surface of the downstream volume elements was assumed to be equal to the initial air temperature plus the temperature rise calculated from equation (12). The air temperature used for the middle surfaces was the average of the air temperature used on the ends. The results of these assumptions agreed well with experimental observations.

A 16 element model was programmed, but its solution for average concentrate temperature varied only about 1°F from the 9 element model after a 30°F temperature change. Also, the time step needed for stability did not change. The 9 element model was chosen for the parameter study because it used about 25% less computer time.

The final model could predict the temperature distribution in cans of concentrate versus time in the tunnel. Time in the tunnel is related to position in the tunnel by the tunnel length and the average conveyor belt speed. The model was used primarily to predict concentrate freezing times for various values of upstream air temperature T_a , initial concentrate temperature, T_i , convective heat transfer coefficient, h , can height and radius, and concentrate thermal properties.

CHAPTER 3
MEASUREMENTS

3.1 MEASUREMENTS

A variety of measurements were necessary to evaluate the accuracy of the computer model, and to determine the tunnel's typical operating conditions. Measurements of the tunnel's internal operating conditions were complicated by the harsh environment created inside the tunnel. Also, the concentrate can size and average conveyor belt speed varied with production requirements. To simplify measurement problems, data was only recorded for the 12 ounce can size, which was the most frequent size cooled in the tunnel.

3.2 PRODUCTION RATE

The production rate, considered here as the mass flow rate of concentrate through the tunnel, depends on the average conveyor belt speed and the void fraction, ϵ . Although the conveyor belt drive was a constant speed drive, it was occasionally turned off and on due to production requirements. An average conveyor belt speed was estimated by noting the time required for a given can to go from entrance to exit of the tunnel. The average speed varied between 60 and 80 ft/hr.

The void fraction was estimated by using installed counters. Immediately after exiting the freeze tunnel, the cans were packed in boxes. Installed counters displayed the number of boxes that had been produced. The number of cans exiting the tunnel during the time required for a given can to pass from entrance to exit of the tunnel, was calculated from the counter readings. The bed volume was assumed to be

one can height tall, and as long and as wide as the conveyor belt inside the tunnel. Since, the mass and volume per can was chosen, the ϵ could be estimated as

$$\epsilon = 1 - \frac{(\# \text{ cans per bed})(\text{volume per can})}{(\text{bed volume})}$$

It was found that ϵ typically varied between 0.4 and 0.5. An average value of 0.45 was estimated for the parameter study.

3.3 AIR FLOW RATE

It is necessary to determine the characteristic air velocity in the packed bed to predict a convective heat transfer coefficient. Figure 3 is a simple sketch of the tunnel air flow. Cold air is blown by 10 fans operating in parallel, through the mesh conveyor belt and the bed of concentrate cans. The air then flows through 8 evaporators operating in parallel, and returns to the fan suction. The fans were not spaced evenly along the length of the tunnel and the air velocities in the bed were higher near the ends of the tunnel than near the middle.

The average volumetric flow rate of air through each fan, Q_f , was estimated. Air velocities approaching 100 mph with air temperatures of about -20°F precluded involved or time consuming measurements in the vicinity of the fans. A pitot-static tube and an inclined oil manometer were used to measure the radial velocity distributions in the fan suction. It would have been more desirable to work on the discharge side of the fans, for safety reasons, but the fan discharge was not accessible during freeze tunnel operation due to the tunnel construction. Data were obtained for values of velocity and radial location along horizontal and vertical radials of several fan suction. Data

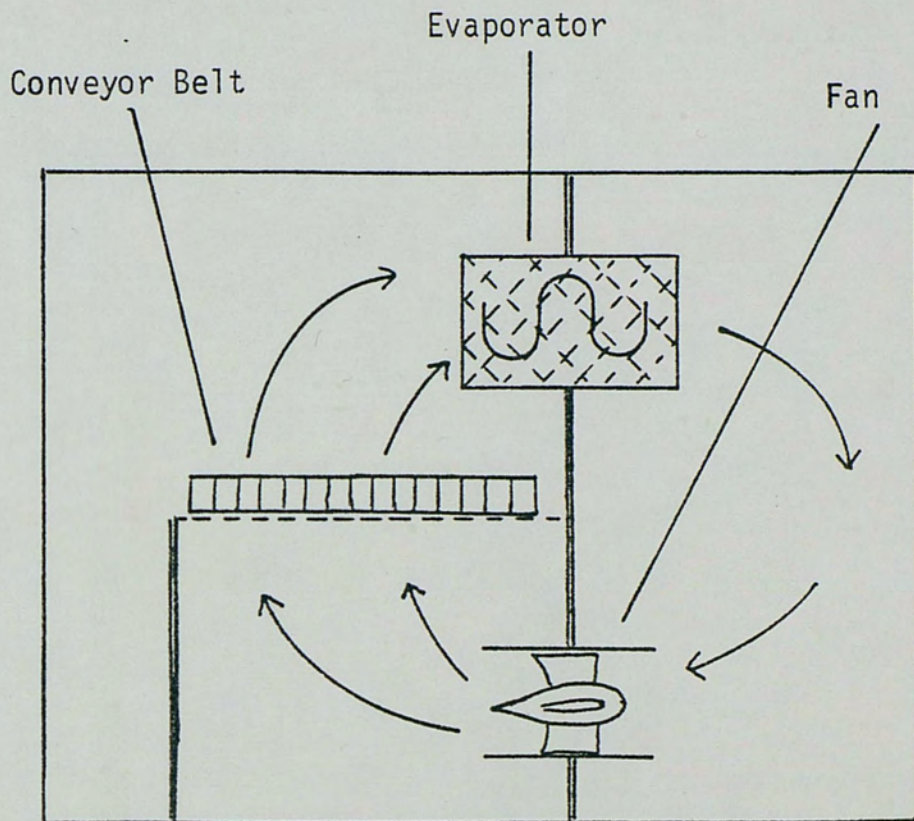


Fig. 3. Freeze Tunnel Air Flow Sketch

for at least 4 values of velocity and radial position were recorded for each radial considered.

The velocities measured were graphically integrated over the cross-sectional area of a fan suction to determine the volumetric flow rate per fan [12]

$$Q_f = \int u dA$$

The average flow rate per fan was approximately 24,000 cfm. By assuming uniform flow, the characteristic velocity, u^* , of the packed bed can be estimated for equation (10).

$$u^* = Q/\epsilon A$$

Then, u^* would be approximately 6 ft/sec.

Attempts were also made to measure the velocity distribution of the bed by directly measuring velocity in the void spaces, over the cross-sectional area of the bed. The manometer could not be used because the bed was in motion, and no level surfaces existed to put it on. A styro-foam ball type of flow detector was used with some success. Although the lower air velocities, in the larger void spaces, were below the detector's minimum sensitivity, it would consistently indicate the air velocities in the void spaces in the tightly packed regions of the bed. When averaged over the length of the tunnel, and corrected for temperature, the peak air velocity was approximately 9 ft/sec. This, of course, is not u^* but can be used to approximate its value.

When observed from above, the packed bed appears to consist of regions of tightly packed cans separated by small, relatively empty gaps. This observation suggested a way to use the peak air velocity to pre-

dict u^* . The bed is considered to consist of two types of areas, one of tightly packed cans and the other of no cans at all, such that

$$A_{\text{void}} = A_1 + A_2$$

where

subscript 1 = refers to the tight packed region

subscript 2 = refers to the region of no cans

Then equation (9) becomes

$$u^* = \frac{1}{A_{\text{void}}} \int u_1 dA_1 + \frac{1}{A_{\text{void}}} \int u_2 dA_2 \quad (13)$$

The values of A_1 and A_2 can be estimated from ϵ data. As previously discussed, on the average, $\epsilon = 0.45$ for the tunnel. In the open regions, $\epsilon_2 = 1.0$ by definition. The value of ϵ in the tight packed region can be estimated from the tightest observed packing geometry as viewed from directly above the bed. Neglecting the edges of the region, every void space is surrounded by 3 cans and every can is surrounded by 6 void spaces. By observation the smallest unit of area that is characterized by a void fraction typical of the region, would be a triangular region, as sketched in figure 4. The length of each side is equal to twice the radius of a can. The equilateral triangle is drawn between the centers of any three adjacent cans. The minimum void fraction, ϵ_1 , expected can be analytically or graphically estimated and is approximately 0.09. Of course, when ϵ_1 and ϵ_2 are averaged over the area of the bed, the average ϵ must be 0.45 as previously determined,

$$\epsilon = (\epsilon_1 A_1 + \epsilon_2 A_2) / A_{\text{void}}$$

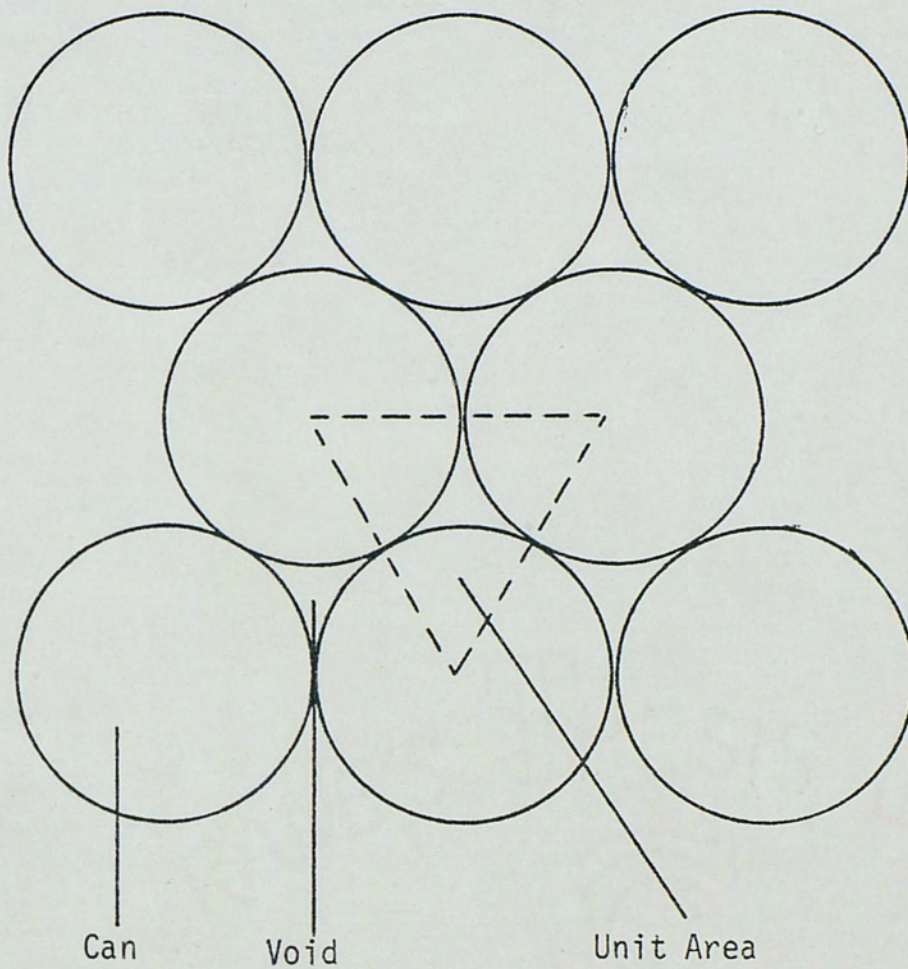


Fig. 4. Top View of Observed Packing Arrangement

Also

$$(A_1 + A_2) / A_{\text{void}} = 1$$

Combining the last two equations, eliminating A_2 , setting $\epsilon_2 = 1.0$ and solving the A_1 results in

$$A_1 / A_{\text{void}} = (1 - \epsilon) / (1 - \epsilon_1)$$

Finally, equation (13) can be used to estimate u^* . Values for A_1 / A_{void} and A_2 / A_{void} are determined from the equation and ϵ data above. A value for u_1 was measured. But the value of u_2 was below the minimum detectable velocity for the detector used. The temperature corrected minimum detectable velocity was approximately 1.3 ft/sec. When u_2 is assumed to have a value between 0.0 and 1.3 ft/sec, a value for u^* between 5.5 and 6.0 ft/sec results respectively. This result agrees with the value of 6.0 ft/sec resulting from the fan data.

3.4 TEMPERATURES

The average concentrate temperature was measured as a function of time and position in the freeze tunnel. Also, the air temperature upstream and downstream of the concentrate cans was measured as a function of position in the tunnel. These temperatures were measured with laboratory grade or precision grade mercury thermometers. Either partial or total immersion thermometers were used, as required by the measurement.

The steady state air temperatures were relatively consistent. The air temperature averaged -20°F upstream of the concentrate. The downstream air temperature varied with position in the tunnel. Near the entrance of the tunnel, the downstream air averaged -2°F , while at the exit the downstream air temperature averaged -15°F . However, necessary

evaporator defrosting did temporarily affect the air temperatures.

Evaporator defrosting occurred automatically for 1 evaporator every 3 hours. They were defrosted with hot gas. Hydraulically operated louvers were designed to automatically shut and isolate each evaporator during its defrost cycle and then open for normal operation. However, the louver system did not operate properly during the time period in which data was taken. The louvers remained open, or partially open, during defrost periods. Air temperatures downstream of a defrosting evaporator were observed to reach 30°F. This, of course, also affected the concentrate temperatures. Although it was attempted, taking data during defrosting periods could not be avoided because of the volume of data needed to establish typical operating conditions. Also, it usually took between 2.0 and 2.5 hours for a can of concentrate to go from tunnel entrance to exit so that most cans were subjected to a defrost cycle, which occurred every 3 hours.

Measuring the average temperature of a cylindrical concentrate can in a freeze tunnel is difficult. The major difficulty is caused by the large temperature gradient that results from the rapid freezing process. In some cases a can of concentrate, partway through the tunnel may be frozen solid near its surface, and still be liquid in the middle. Two methods were used to approximate the typical average temperature of the concentrate versus time and distance in the tunnel.

One method used to approximate the concentrate temperature, referred to as mixing cup method, was to empty selected cans into prechilled thermos bottles. The concentrate was then mechanically mixed until its

temperature was uniform enough to be measured with a single thermometer. However, the frozen concentrate was usually too hard to be easily mixed. Taking too much time or expending too much work mixing the concentrate was found to affect the concentrate temperature. A standard routine was established to expeditiously mix the concentrate. The routine sometimes left temperature variations within the concentrate of about 2F, but further mixing could also produce a comparable variation in the temperature. This measurement uncertainty contributed to some of the data scatter, primarily in the well frozen cans that had been in the tunnel over an hour. Data were collected by removing cans from specific locations in the tunnel and recording their temperatures. The average conveyor belt speed was measured and used to estimate the time the cans had been in the tunnel based on their positions. Data were collected several times on different days so that typical values could be determined. The actual data points obtained are plotted in figure 5 versus time in the freeze tunnel. The plot is dimensionless with the dimensionless temperature, θ defined as

$$\theta = \frac{T - T_a}{T_i - T_a}$$

where

T_i = the average initial concentrate temperature

T_a = the air temperature upstream of the concentrate
and the dimensionless time, \bar{t} , defined as

$$\bar{t} = t/t_0$$

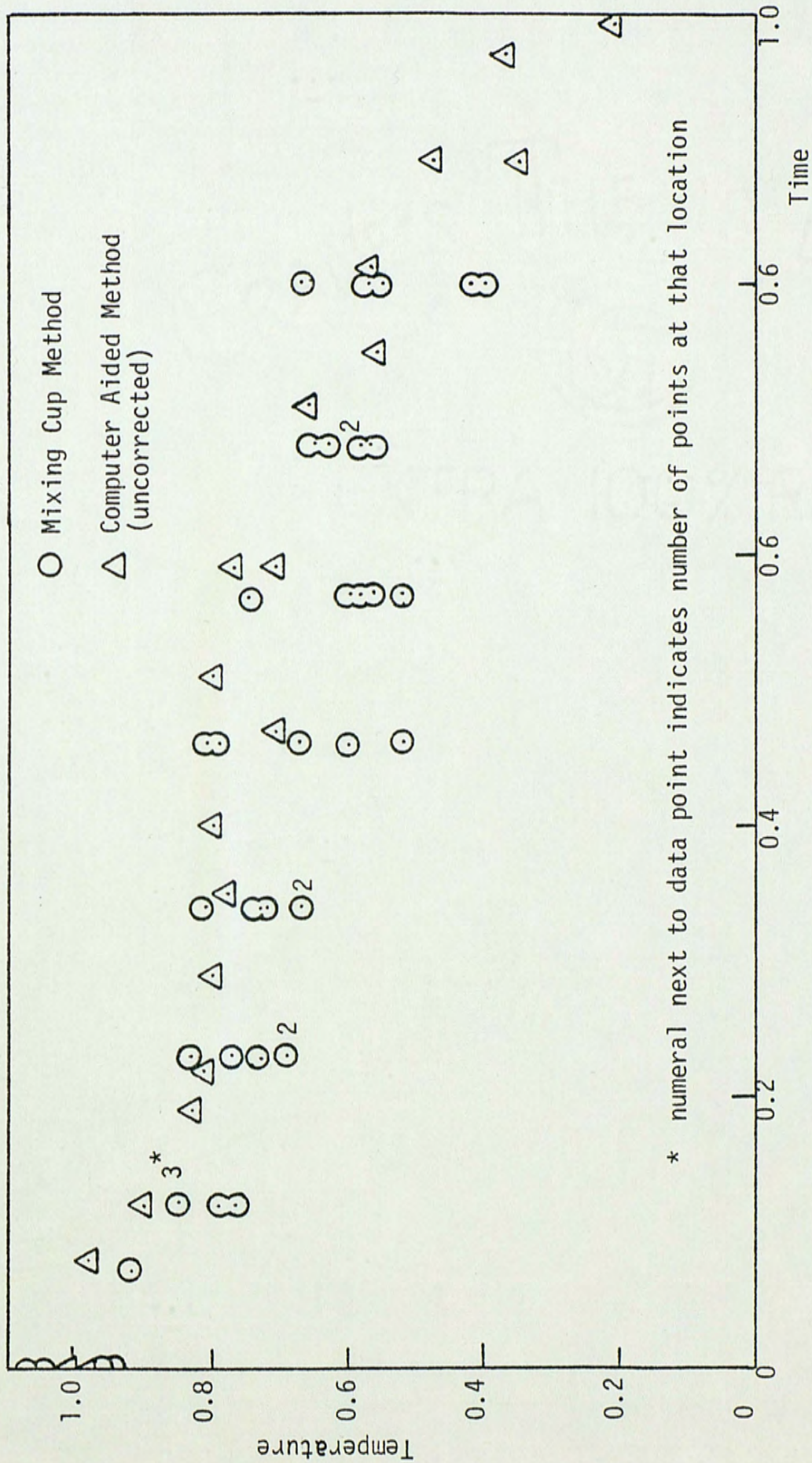


Fig. 5. Temperature Data

where

t_0 = the reference time

In this case

$T_i = 28^\circ\text{F}$

$T_a = -20^\circ\text{F}$

$t_0 = 2.5 \text{ hr}$

The data scatter is due to a variety of reasons. Variations in initial concentrate temperature, measurement uncertainties, evaporators defrosting at different locations, variation in air flow rates between different regions of the tunnel and the stop and go operation of the conveyor belt are all contributors to the data scatter. However, the temperatures do generally decrease as expected. The average value of these data points is graphed versus time in the tunnel in figure 6. The average concentrate temperature decreases more slowly in the middle of the tunnel than near the ends. This is expected because of the higher effective specific heat capacity of the concentrate at temperatures typical of those in the middle of the tunnel and also because of the higher air velocities near the ends of the tunnel.

A different method for determining the average concentrate temperature was also used and is referred to as the computer aided method for discussion purposes. A hole was punched in the center of several can tops at the tunnel entrance. Mercury thermometers were then inserted in the cans of concentrate. Washers were taped to the thermometers to hold them at the proper immersion depth. The

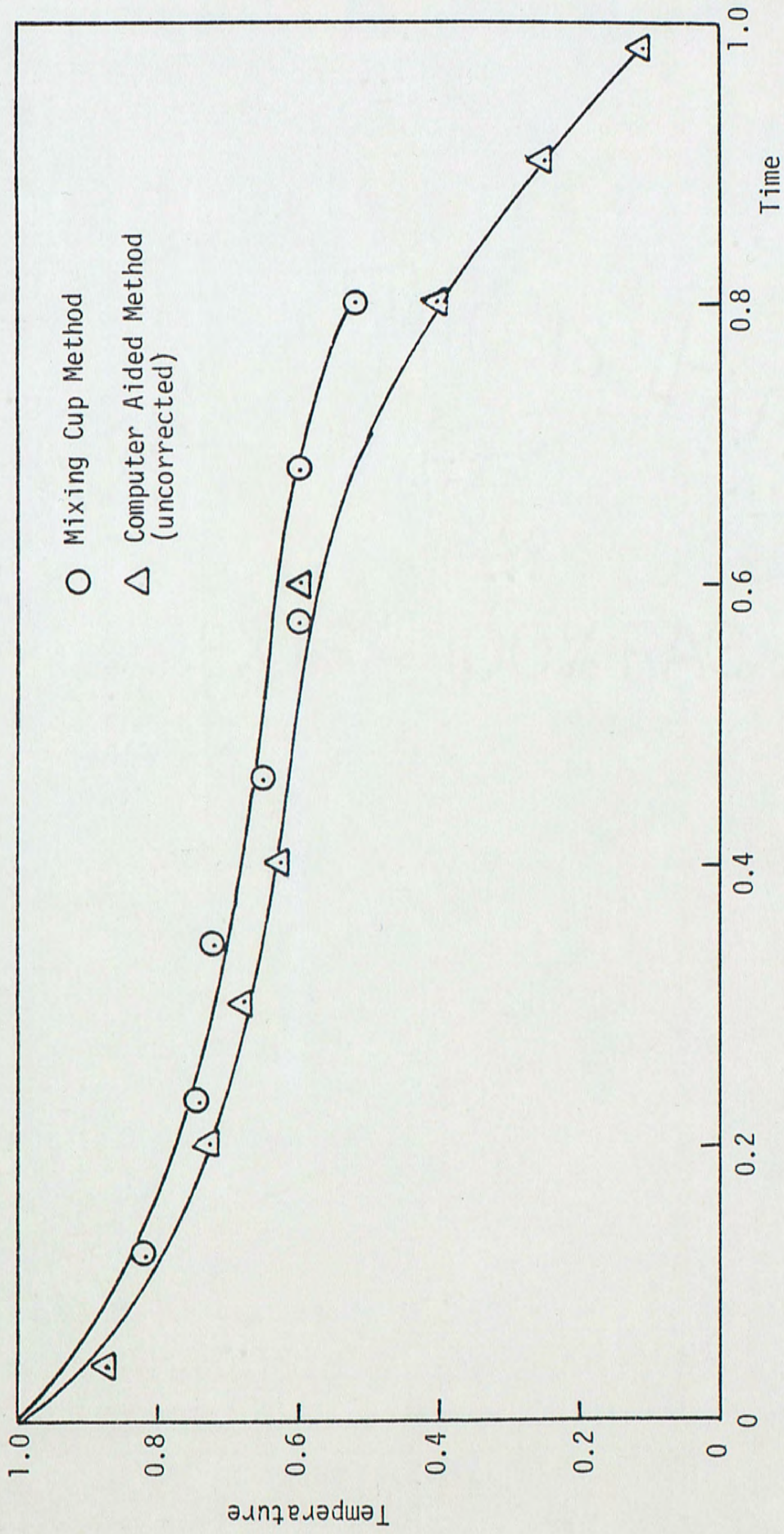


Fig. 6. Average Temperature of Concentrate vs. Time in the Freeze Tunnel

temperatures indicated, and time of the readings, were recorded periodically as the cans progressed through the tunnel. The resulting data is also plotted in figure 5. Each data point is an average of the several thermometer readings recorded each time. These temperatures are not the average concentrate temperatures, but instead, the concentrate temperature at the can's centerline, near the thermometer's mercury bulb.

These thermometer readings were used to estimate the average concentrate temperature with the aid of the computer model. The computer could predict the average temperature and the temperature at 9 nodal locations in a can of concentrate as a function of time for any value of heat transfer coefficient, air temperature, initial concentrate temperature, and can size. All parameters of the computer model were set to the best estimated conditions in the tunnel. Values for the average temperature and the temperatures at the 3 centerline nodal positions were determined as function of time with the computer. Temperatures at the centerline nodal positions were used to obtain approximate graphs of temperature versus height at the can's centerline. The graphs were used to average the centerline temperature over the heights occupied by the mercury bulb. Comparing the predicted results with the measured results shows an average difference of less than 2.0°F between the computer prediction and the measured center line temperatures for 2 hours of cooling. It was assumed the difference between the centerline temperature around the mercury bulb, predicted from the computer results, and the

computer predicted average temperature for the can was equal to the difference between the measured centerline temperature and the actual average temperature. By adding this temperature difference to the measured centerline temperature an estimate of the corresponding average temperature was obtained. The temperature difference varied with time so the procedure was repeated for different times. A plot of the results of this computer aided method is contained in figure 6, along with the results of the mixing cup method. The dimensionless values are defined as in the mixing cup method, except that the average initial concentrate temperature was measured as 25°F rather than 28°F.

Comparing the graphs in figure 6 shows close agreement except at times near the end of the tunnel. The computer aided graph is longer because the average conveyor belt speed was slower when that data was recorded, and the cans were in the tunnel longer. The largest temperature difference between methods occurs at the end of the mixing cup curve, when the cans were near the tunnel exit. During periodic checks of the temperature of concentrate exiting the tunnel temperature differences this large were observed as a result of the routine operation of the tunnel. However, another possible factor in this discrepancy is that when data was recorded for the mixing cup curve the freeze tunnel door was open longer, as thermos bottles were passed in and out, than when thermos bottles were not used and only a data taker went in and out. The freeze tunnel door was large and when open could significantly increase

the cooling load resulting in generally higher temperatures.

A final note on concentrate temperatures tends to agree equally with the results of both the mixing cup method and the computer aided method. The operators of the freeze tunnel set up its operation to produce a nominal concentrate outlet temperature of 0.0°F. Concentrate is normally stored in the 0.0F to -5.0°F temperature range.

3.5 AVERAGE NUSSOLT NUMBER

One initial use of the measurements is to evaluate the accuracy of and improve the precision of the computer model. Many of the parameters in the model, such as u^* , the packed bed characteristic velocity and the typical void fraction, could only be obtained by measurements.

The typical heat transfer coefficient and Nusselt number for the freeze tunnel can now be estimated based on the correlation in Section 2.3. For the 12 ounce can size (0.104 ft in radius and 0.375 ft in height), measured air temperatures, a characteristic velocity of 6 ft/sec, and a void fraction of 0.45, the correlation predicts a heat transfer coefficient and Nusselt number of about

$$h = 8.2 \text{ Btu/hr ft}^2\text{°F}$$

$$\text{Nu} = 126.0$$

The accuracy of the correlation is better than $\pm 25\%$ [10]. Of course, the graphs of concentrate temperature versus time can also be used to measure h .

The computer is needed to estimate h from the temperature

measurements. This can be done by simulating the existing conditions in the tunnel as closely as possible, and then varying h until the computer predicted temperatures are approximately equal to the measured temperatures. Simulating conditions in the tunnel required varying u^* and h in different regions of the tunnel, to account for the uneven fan distribution, and also required simulating evaporator defrosting. Varying h was accomplished by dividing the tunnel into three regions, a region of low u^* and h in the middle, and two regions of high u^* and h at the ends of the tunnel. It was assumed u^* was approximately 50% greater in the first 15% and the last 15% of the tunnel based on the measurements of the void space air velocities. To simulate the louver malfunction based on measured values, it was assumed that after 1 hour of cooling the upstream air temperature increased to 30°F for about 10 minutes and then returned to its original value of -20°F. The resulting predictions of average concentrate temperature versus time for various h and Nu is graphed in figure 7 along with the measured values.

Comparison of these curves shows the computer aided curve is very close to the curve for the average h and Nu predicted from the packed bed correlation. The mixing cup curve appears to be closer to a Nu of 86, even when some deviation is allowed to account for door openings. The average over the length of the tunnel of the two measured curves is close to the curve resulting from a Nu of 101. To be conservative, the tunnel's typical Nu was assumed to be 101 for the purposes of the parameter study. This value is

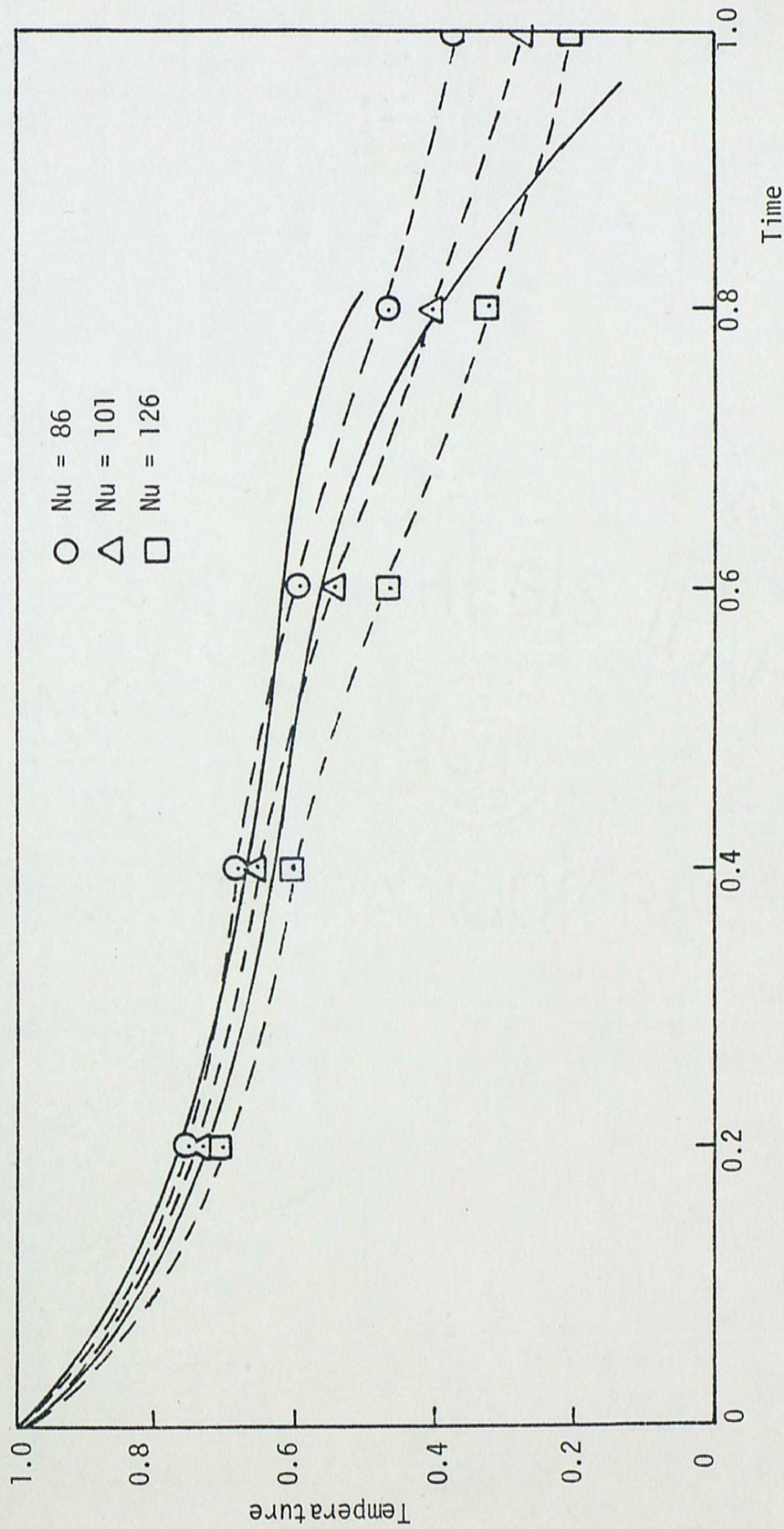


Fig. 7. Comparison of Measured and Computer Predicted Values of the Average Temperature of Concentrate vs. Time in the Freeze Tunnel

20% lower than the value predicted by the packed bed correlation. This accuracy is acceptable for an initial parameter study. A more accurate evaluation would require more temperature data or another method of evaluating the concentrate temperature.

3.6 IMPLICATIONS OF THE MEASUREMENTS ON THE PARAMETER STUDY

The measurements can be used to estimate the relative contributions of each factor in the tunnel energy balance. Any factor affecting the cooling load will affect the tunnel's coefficient of performance and the parameter study. Evaluation of each factor will help indicate the importance and potential of each factor to the efficient operation of the tunnel. Recalling from Section 2.1, the equations for the tunnel coefficient of performance and the tunnel energy balance are

$$\text{COP}_t = q_c / (q_L / \text{COP} + W_f) \quad (4)$$

$$q_L = q_c + q_{\text{trans}} + q_{\text{inf}} + q_f \quad (2)$$

where

COP_t = tunnel coefficient of performance

q_c = heat removal rate from the concentrate

q_L = cooling load

q_{trans} = transmission heat gain

q_{inf} = infiltration heat gain

q_f = fan heat gain

COP = coefficient of performance for the refrigeration plant

Calculation of the COP is discussed in Section 4.2. The other terms can be calculated using equations from Chapter 2, tunnel dimensions from

figure 1 , and data from Chapter 3. A summary of the tunnel's typical operating conditions is contained in table 2. Using this information, the energy consumption can be calculated.

The heat removal rate from the concentrate is calculated by

$$q_c = \dot{m} \int_{T_i}^{T_f} c_{ef} dT \quad (5)$$

When the integral is evaluated between 28°F and 0°F by graphically integrating the values in Table 2.1, the result is

$$\int_0^{28} c_{ef} dT = 58.0 \text{ Btu/lbm}$$

The mass flow rate of the concentrate can be found using

$$\dot{m} = S W H (1-\epsilon)\rho$$

where

S = conveyor belt speed

W = packed bed or conveyor belt width

H = packed bed height

ρ = average concentrate density

The average concentrate density, ρ , was graphically averaged between 28°F and 0°F and is approximately 74 lbm/ft³. Using this information

$$q_c = 6.20 \times 10^5 \text{ Btu/hr}$$

The transmission heat gain is calculated using data from table 2. For the walls and ceiling the result is

$$q = 2.35 \times 10^4 \text{ Btu/hr}$$

and for the floor the result is

$$q = 2.40 \times 10^4 \text{ Btu/hr}$$

TABLE 2
SUMMARY OF FREEZE TUNNEL CHARACTERISTICS

Tunnel Length	150 ft
Tunnel Width	20 ft
Tunnel Height	15 ft
Conveyor Belt Length	150 ft
Conveyor Belt Width	10 ft
Average Conveyor Belt Speed	70 ft/hr
Packed Bed (can) Height	0.375 ft
Void Fraction	0.45
Door Height	8 ft
Door Width	4 ft
Overall Heat Transfer Coefficient, Walls	0.025 BTU/hr ft ² °F
Overall Heat Transfer Coefficient, Floor	0.1 BTU/hr ft ² °F
Design Wet Bulb Temperature	79°F
Design Dry Bulb Temperature	93°F
Design Ground Temperature	60°F
Initial Concentrate Temperature	28°F
Final Concentrate Temperature	0°F
Freeze Tunnel Air Temperature	-20°F

The total transmission heat gain is

$$q_{\text{trans}} = 4.75 \times 10^4 \text{ Btu/hr}$$

More assumptions are required to calculate q_{inf} . The enthalpy difference between outside air at design temperature and inside air at -20°F , Δh , is approximately 50 Btu/lbm. The cfm infiltrating with the cans is

$$\text{cfm} = S W H \epsilon$$

Using values from table 2 results in a heat gain from infiltration with the conveyor belt of

$$q = 98 \text{ Btu/hr}$$

The infiltration heat gain due to door openings can vary widely.

Assuming the door is open only 15 seconds per hour on the average and using the methods discussed in Section 2.1 results in a heat gain due to door openings of

$$q = 4.50 \times 10^3 \text{ Btu/hr}$$

The total infiltration heat gain is

$$q_{\text{inf}} = 4.60 \times 10^3 \text{ Btu/hr}$$

The heat gain resulting from the fans is

$$q_f = 3.00 \times 10^5 \text{ Btu/hr}$$

The total cooling load from equation (2) is

$$q_L = 9.72 \times 10^5 \text{ Btu/hr}$$

Table 3 is a summary of these results.

The major loads are q_c and q_f while the value of q_{inf} is negligible. The value of q_{trans} is relatively small even as a worst case value. Therefore, for the purposes of the parameter study the cooling load is

TABLE 3
SUMMARY OF COOLING LOADS

Source	Heat Gain (BTU/hr)	Percent of Total
Concentrate	6.20×10^5	63.8
Transmission	4.75×10^4	4.9
Infiltration	4.60×10^3	0.5
Fans	3.00×10^5	30.9
Total	9.72×10^5	100.0

approximated as

$$q_L = q_c + q_f$$

Then, equation (4) becomes

$$\text{COP}_t = \frac{q_c}{(q_c + q_f)/\text{COP} + W_f} \quad (14)$$

CHAPTER 4
THE PARAMETER STUDY

4.1 THE COEFFICIENT OF PERFORMANCE OF THE FREEZE TUNNEL

The equation for COP_t can still be put in a more convenient form for the parameter study. Rearranging the terms in equation (14) results in

$$COP_t = \frac{COP}{1 + (q_f + W_f COP)/q_c}$$

From Chapter 2,

$$q_f = 2995 \text{ hp}$$

where

$$Hp = \text{fan horsepower}$$

Also, using a convenient conversion results in

$$W_f = 2545 \text{ Hp}$$

Substituting these expressions into the COP_t formula results in

$$COP_t = \frac{COP}{1 + (2995 + 2545 COP) \frac{Hp}{q_c}}$$

One more simplifying approximation is to assume this equation can be rewritten

$$COP_t = \frac{COP}{1 + (1+COP)K} \quad (15)$$

In this form, K is a dimensionless number defined as

$$K = \frac{2545 \text{ Hp } \Delta t}{\Delta Q_c}$$

where

ΔQ_c = the nominal heat removed from the concentrate in a full freeze tunnel

Δt = the freezing time or the time required for a can to pass through the freeze tunnel

and

$$q_c = \Delta Q_c / \Delta t$$

K is a ratio of the work done by the fans divided by the useful refrigeration effect. Even before the parameter study, it is easy to see the significance of this ratio. For a given COP, the tunnel is most effective, or the COP_t is a maximum, when

$$K = 0$$

or

$$q_c \gg \dot{W}_f$$

Of course when this occurs, there are essentially no fans in the tunnel and the freeze tunnel has become a refrigerated space. Typically this cannot be accomplished because the freezing times become too long. To obtain the desired freezing times, for a given capacity of the tunnel, fans are added. As K increases, the COP_t decreases. Figure 8 and figure 9 show briefly how COP_t , COP, and K are related.

4.2 VARIATION IN THE COEFFICIENT OF PERFORMANCE OF THE REFRIGERATION PLANT WITH FREEZE TUNNEL AIR TEMPERATURE

The COP for the refrigeration plant associated with the observed freeze tunnel is difficult to accurately calculate. The two stage ammonia vapor compression plant supplies loads other than the freeze tunnel. Some loads are supplied from the intermediate stage. The enthalpy of the refrigerant cannot be estimated for all the important thermodynamic states. For the purposes of the parameter study, the COP was estimated by assuming the refrigerant reaches each compressor as a saturated vapor, compression is isentropic, and the

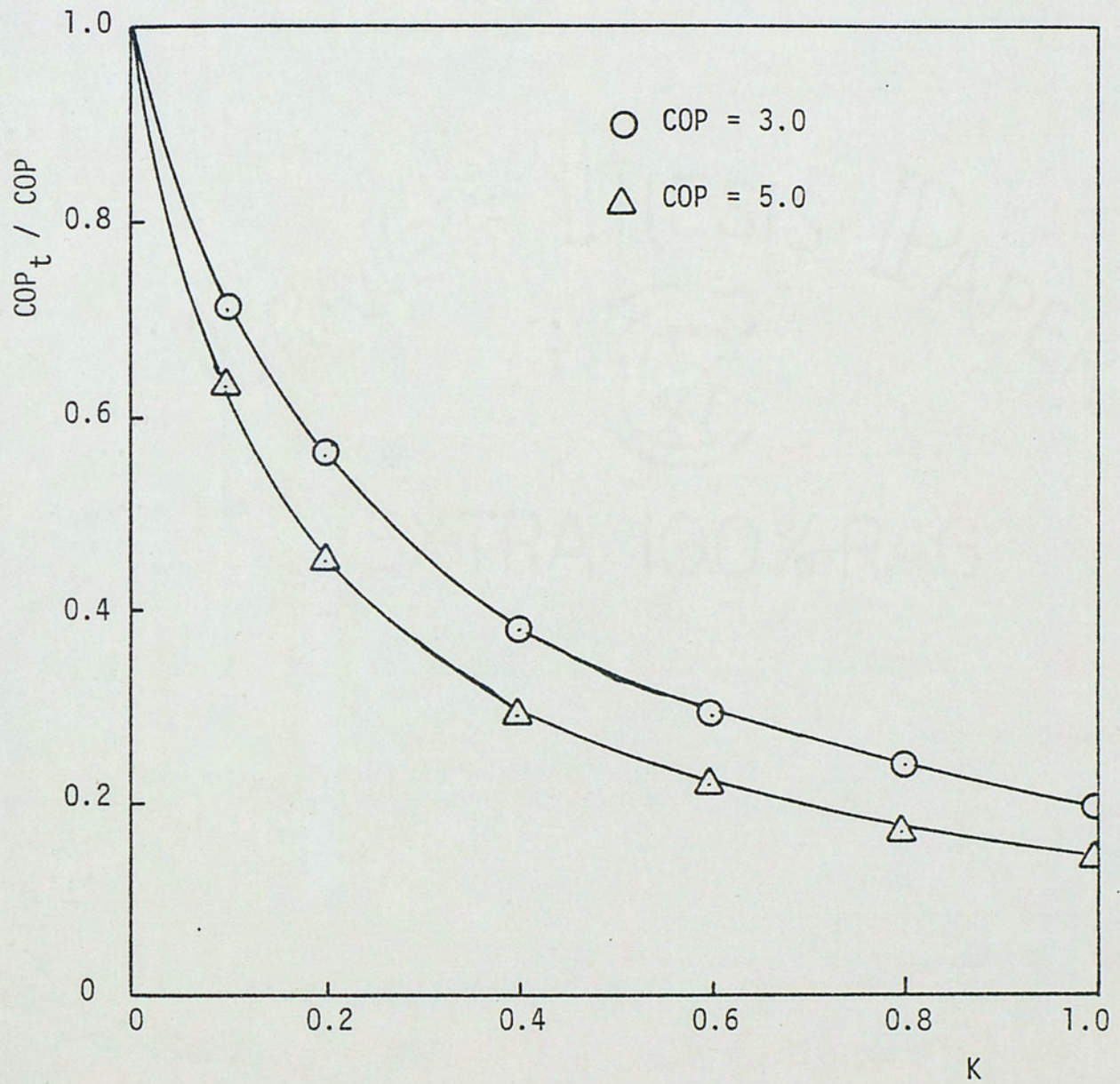


Fig. 8. Freeze Tunnel Coefficient of Performance Divided by the Refrigeration Coefficient of Performance vs. Fan Power Divided by the Useful Refrigeration Effect

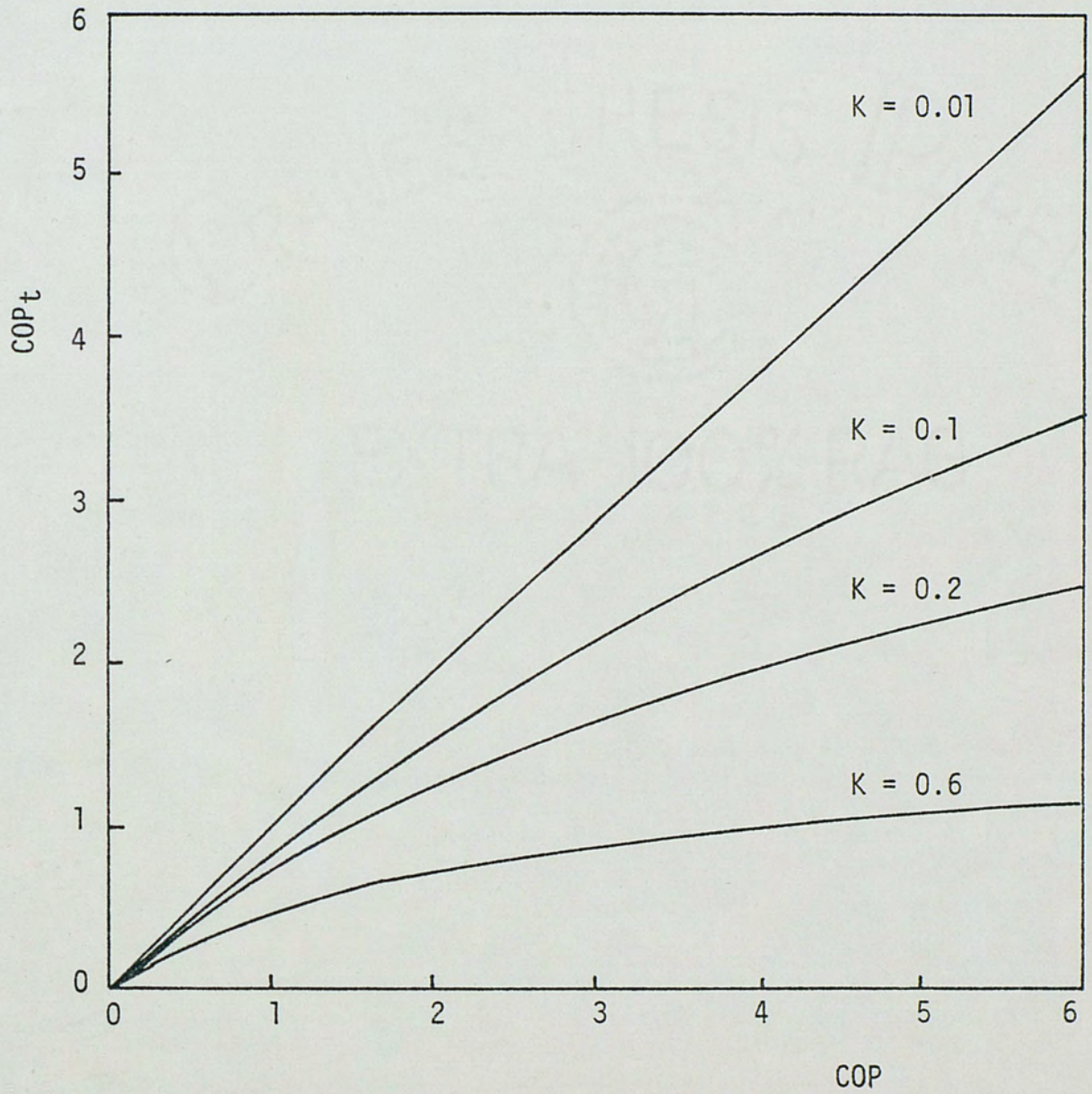


Fig. 9. Freeze Tunnel Coefficient of Performance vs. Refrigeration Unit Coefficient of Performance

minimum enthalpy at any pressure is approximately equal to the enthalpy of saturated liquid refrigerant at the highest pressure in the cycle.

Information has to be obtained concerning operating pressures to calculate the COP to be used in the parameter study. The stage pressures that produce an air temperature in the tunnel of -20°F were observed as

High Pressure	170 psig
Intermediate Pressure	30 psig
Evaporator Pressure	10 inch Hg, vac

The air temperature is a parameter in the study. To change the air temperature the evaporator pressure must be changed, for a given cooling load. This of course affects the COP, so that at every air temperature and evaporator pressure, a new COP must be estimated. As a rough estimate, it was assumed that for a given change in air temperature, the evaporator's saturation temperature must change an equal amount. It was also assumed that the evaporator pressure changes a corresponding amount while the high and intermediate pressures are constant. Using these assumptions, the evaporator pressures needed to produce given air temperatures and the corresponding COP's were estimated. The results are listed in table 4.

4.3 VARIATION IN THE FAN WORK WITH NUSSELT NUMBER

Fan work, W_f , is also an important parameter. W_f is related to the packed bed's characteristic velocity, u^* , and its heat transfer coefficient, h . However, predicting how a change in W_f will affect u^* and h is a difficult problem. Usually detailed know-

TABLE 4

COEFFICIENT OF PERFORMANCE OF THE REFRIGERATION PLANT

COP	Air Temperature (°F)
6.0	-10
5.4	-20
4.9	-30
4.5	-40

ledge of the fan's characteristic curve of pressure head versus volumetric air flow rate is needed, as well as the systems characteristic curve of head loss versus volumetric air flow rate, to accurately estimate a change in a system's operating point [13]. In this case, only 1 operating point is known. The system curve could be determined experimentally, but this would be too difficult. Therefore, for an initial investigation the fan laws [13] were used as a rough approximation for the relationship between W_f and u^* . The applicable fan law in this case, assuming u^* is directly proportional to the volumetric air flow rate, is

$$W_f \propto u^{*3}$$

At the known operating point,

$$W_f = 100 \text{ Hp}$$

$$u^* = 6.0 \text{ ft/sec}$$

$$Nu = 101$$

For a given change in W_f , the fan law can be used to estimate the new u^* . Then the packed bed correlation can be used to calculate the new Nu and h .

4.4 THE FREEZE TUNNEL COEFFICIENT OF PERFORMANCE VERSUS THE NUSSELT NUMBER

In conducting a parameter study for the freeze tunnel under observation, a simplification occurs because ΔQ_c is fixed. Any change in Nu , with a corresponding change in W_f , affects both the COP_t and the freezing time, Δt . The computer model can be used to predict how a change in Nu , or a change in air temperature, T_a , will affect the freezing time. Although the ΔQ_c is fixed, any change in the freezing

time will affect q_c .

The computer was programmed to predict the average concentrate temperature versus time for various values of h and T_a . The time required for the average concentrate temperature to change from an initial value of 28°F to a final value of 0°F , considered the freezing time, was determined from the computer output. Then the COP_t was calculated for each value of h and T_a , or equivalently, Nu and T_a . For every value of T_a , the estimated COP from Table 4 was used to estimate COP_t . The fan horsepower, Hp , was estimated for each value of h and Nu , by using the fan law discussed in Section 4.3, relative to the known operating conditions. Since Hp , ΔQ_c , and Δt are known at each point, K may also be calculated. A summary of the results is graphed in Figure 10 and figure 11.

Figure 10 is a graph of COP_t/COP versus Nu . The ratio of COP_t/COP has a maximum value of 1.0. When COP_t equals COP, the least energy is expended for a given useful refrigeration effect, q_c . Freeze tunnels are operated with lower efficiencies when it is necessary to provide a high q_c and/or a short freezing time, Δt . When heat transfer is increased by using fans to increase the Nu and the ratio of fan work divided by useful refrigeration effect K , increases, then COP_t becomes less than COP. This relationship is displayed by equation (15) as well as figure 10.

Figure 11 is more informative because it shows more clearly how the relationship between COP_t and Nu is affected by T_a . At very low Nu , an increase in T_a also increases the COP_t . This is because

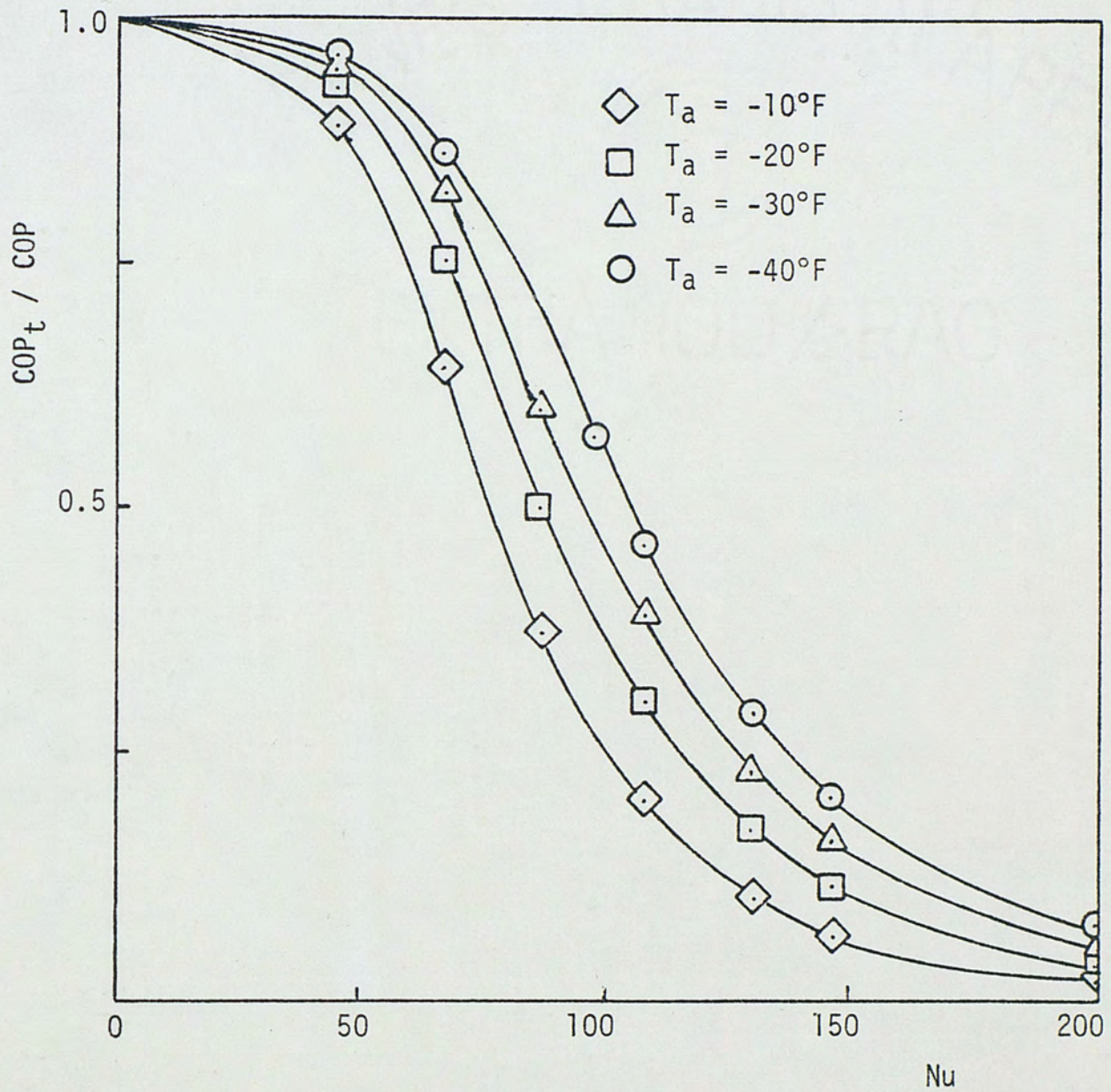


Fig. 10. Freeze Tunnel Coefficient of Performance Divided by the Refrigeration Unit Coefficient of Performance vs. the Nusselt Number

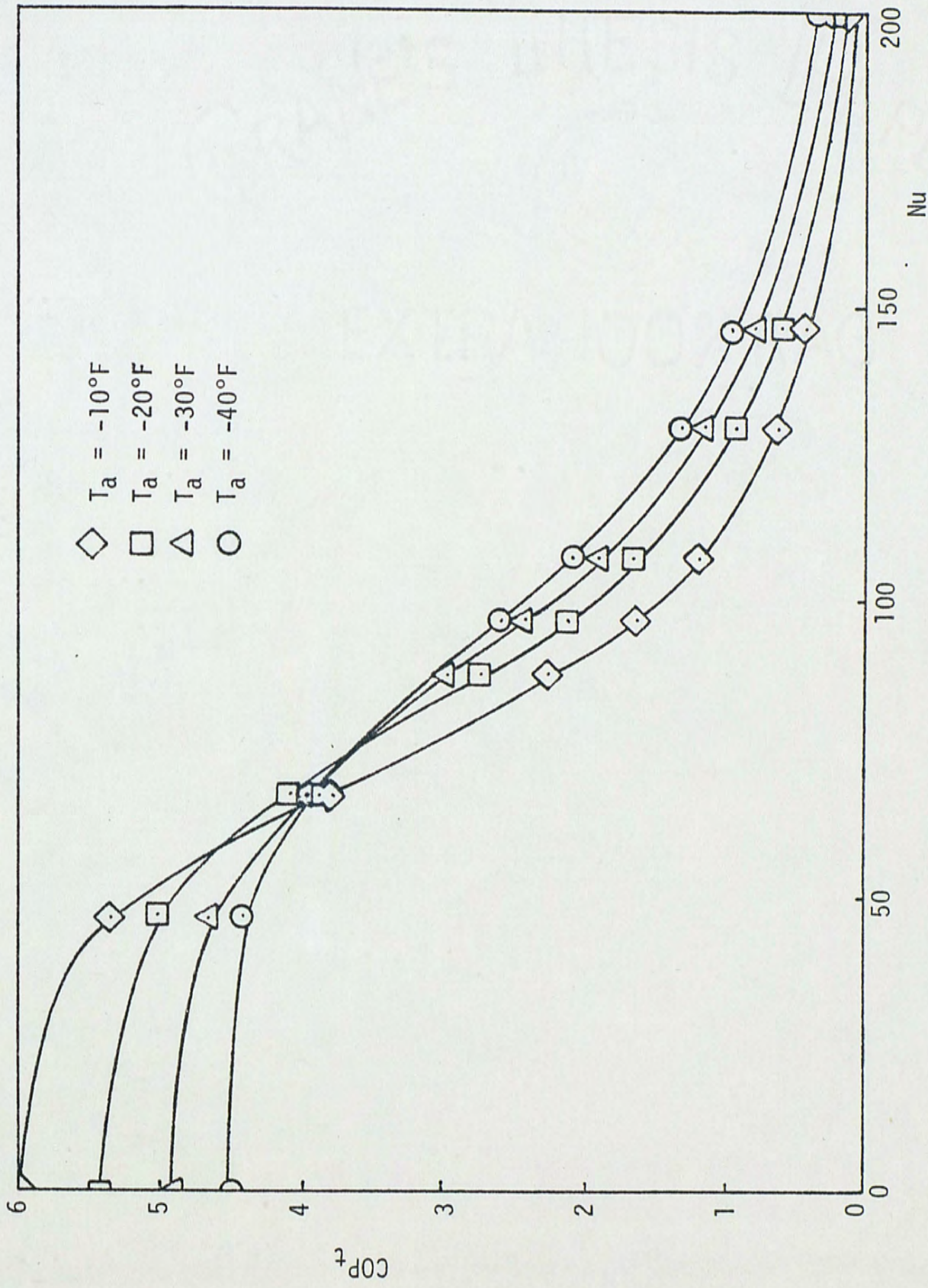


Fig. 11. Freeze Tunnel Coefficient of Performance vs. the Nusselt Number

at low Nu , the system is closer to a refrigerated space than a freeze tunnel and the dominant effect of increasing T_a is the corresponding increase in COP. But at high Nu , the dominant effect of an increase in T_a is increased freezing time, and the COP_t actually decreases. This seems to suggest that while maintaining a higher T_a in a refrigerated space results in higher a COP and lower energy consumption in a refrigeration problem, in a freeze tunnel problem maintaining a higher T_a results in a lower COP_t and higher energy consumption. Also, the COP_t decreases rapidly as K increases, as expected.

4.5 THE FREEZE TUNNEL COEFFICIENT OF PERFORMANCE VERSUS FREEZE TUNNEL CAPACITY

The result of adding fans to a refrigerated space is to increase the rate of heat transfer. This increase in the rate of heat transfer increases the tunnels capacity, q_c , and for a given tunnel size decreases the freezing time. The price of the increased capacity is a decrease in COP_t . The relationship between COP_t and q_c for the observed tunnel is easy to determine at this point.

As a result of Section 4.4, values of COP_t , Nu , T_a , K , and freezing time, Δt , have already been estimated for a variety of computer simulated operating points. Since ΔQ_c is fixed, and a relationship between COP_t and Δt has been established, values of COP_t versus q_c can be generated from

$$q_c = \Delta Q_c / \Delta t$$

Figure 12 is a graph of COP_t versus q_c for the range of Nu

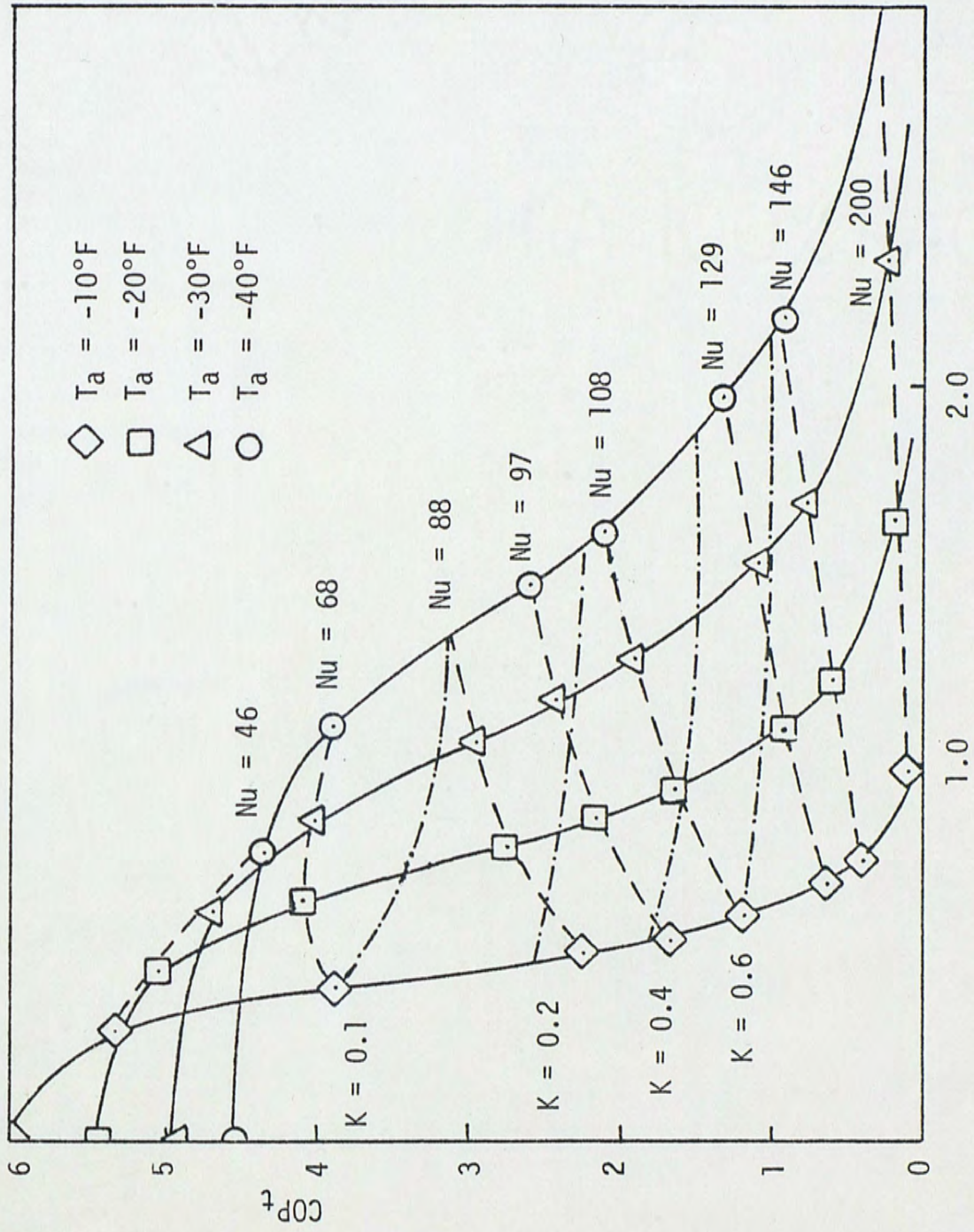


Fig. 12. Freeze Tunnel Coefficient of Performance vs. Freeze Tunnel Capacity

and T_a investigated. The graph displays the important trends discovered in the previous graphs: the highest COP_t is obtained for the lowest values of K and Nu , and for high values of the Nu , the highest COP_t is obtained for the lowest value of T_a . But it also shows that large values of K restrict the tunnel to relatively low COP_t 's, for any value of T_a .

The highest COP_t 's exist at the lowest Nu as expected. But relatively large capacities appear possible even for the lowest Nu investigated. The COP_t of the tunnel is high for low Nu primarily because K is so low. K was calculated using the fan H_p predicted by the fan laws [13]. For a $Nu = 46$, the fan law predicts a $H_p=2$ horsepower, relative to 100 horsepower for a $Nu=101$ as discussed in Section 4.3. Actually producing a significant cooling air flow in a freeze tunnel similar to the one observed with only 2 horsepower may not be achievable because of the physical size and flow characteristics of the evaporators and packed bed. Careful experimental analysis using system and fan curves [13] would be necessary to accurately predict behavior for any conditions significantly different from the measured conditions.

4.6 ENERGY COSTS VERSUS FREEZE TUNNEL CAPACITY

Considering the effects of various values of Nu , T_a and K on the COP_t is important because the COP_t is a measure of the tunnel's effectiveness. But a more obvious method of judging freeze tunnel performance is to consider its energy consumption per unit of processed food. The energy consumed, or equivalently the net work

expended, is related to q_c by the definition of COP_t from equation (1)

$$W_c + W_f = q_c / COP_t$$

The monetary cost of the electricity to operate the tunnel is related to the work performed by

$$d = R q_c / COP_t$$

where

$$d = \text{hourly charge}$$

$$R = \text{cost per unit energy}$$

The unit monetary cost, or cost per unit of food processed is

$$D = d \Delta t = R Q / COP_t$$

where

$$D = \text{unit cost}$$

$$\Delta t = \text{freezing time}$$

$$Q = \text{heat removed per unit food product}$$

Figure 13 is a graph of hourly energy costs, and rate of energy consumption, versus capacity. Once again, except at low capacities, the least energy is expended for a given production rate at the lowest achievable values of Nu , K , and T_a . As the capacity is increased by lowering T_a or increasing Nu the costs increase. However, increased costs may be acceptable or even desirable if the increased capacity results in a decreased unit cost.

The unit costs, both in energy and money is graphed versus capacity in figure 14. This graph displays all the trends noted previously. The most useful new information displayed in this

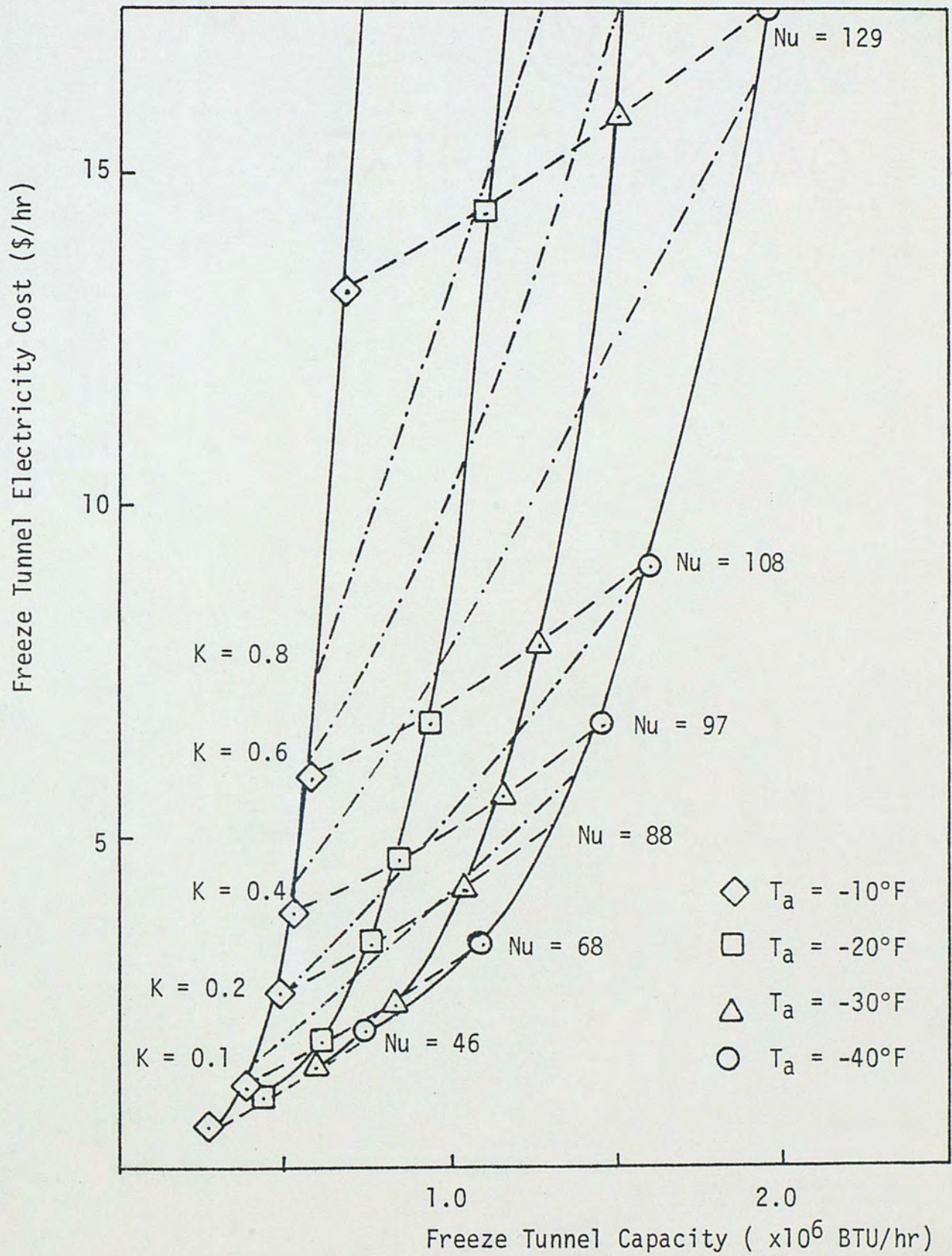


Fig. 13. Freeze Tunnel Electricity Cost vs. Freeze Tunnel Capacity

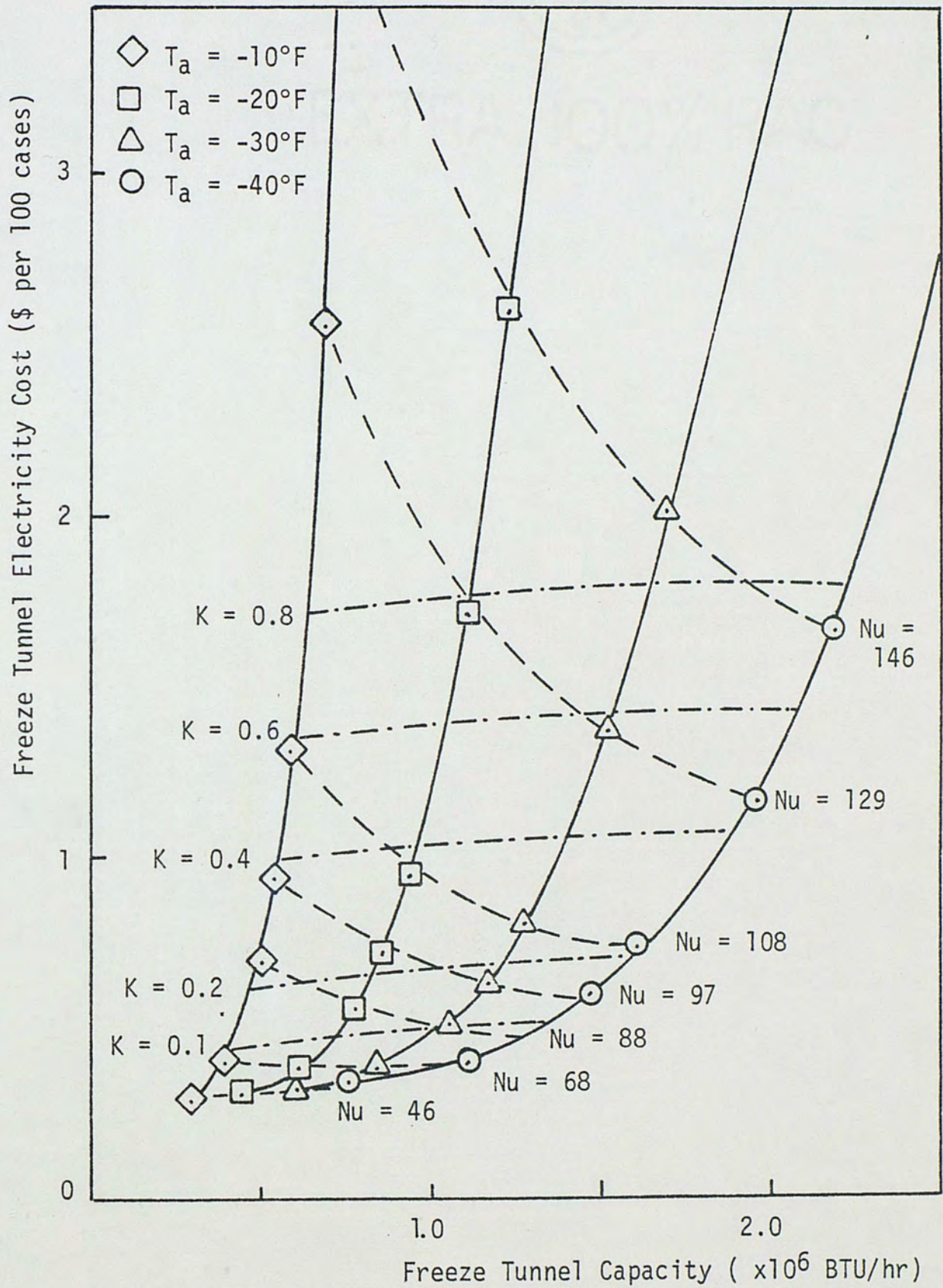


Fig. 14. Freeze Tunnel Electricity Cost per Unit Processed vs. Freeze Tunnel Capacity

graph is that the ratio of the fan work divided by the tunnel capacity, K , can be related approximately to the unit cost of the product. Also, the unit cost and K can be substantially reduced, for a given N_u by lowering T_a .

4.7 RESULTS CONCERNING THE OBSERVED FREEZE TUNNEL

The parameter study applies directly to the observed freeze tunnel with the 12 ounce can size. However, the operating conditions measured in the tunnel reflected the malfunctioning defrosting louvers that resulted in less efficient operation than should occur nominally. The typical operating conditions from section 3.6 result in

$$K = 0.36$$

for an average N_u of 101. The corresponding freezing time was about 1.9 hours. However, freezing times were observed to vary from approximately 1.7 hours up to 2.5 hours depending on day to day operating conditions. As a result K varies from 0.33 to 0.48. This wide variation makes it difficult to predict the tunnel's COP_t or energy costs at a given time. In this case, with a COP of 5.4 for a corresponding air temperature of -20F, the COP_t is 1.33 for a K of 0.33, and the COP_t is 1.74 for a K of 4.8. The variation in the COP_t is about $\pm 11\%$ from its average value of 1.5.

When the defrost cycle is left out of the computer program, and the air temperature T_a is constant at -20F, the predicted freezing time for a Nu of 101 is about 1.6 hours. Then,

$$K = 0.31$$

$$\text{COP}_t = 1.8$$

For any of these operating points, figure 14 predicts a lower cost if the tunnel is operated with colder air temperatures and a smaller Nu , or less fans. For example, assume that the tunnel already operates at its highest expected efficiency with

$$T_a = -20^\circ\text{F}$$

$$Nu = 101$$

$$K = 0.31$$

$$\text{COP}_t = 1.8$$

Figure 14 predicts for that operating condition a unit cost of approximately \$0.80 per 100 cases. Each case contains 24 cans of the 12 fluid ounce size. Figure 14 also predicts that when

$$T_a = -25^\circ\text{F}$$

$$Nu = 90$$

the unit cost is \$0.55 per 100 cases, a savings of about 30%. Using the fan law discussed in Section 4.3, only about 50 Hp in fans is required to produce $Nu = 90$. This is half the fans currently in the tunnel. Although the unit energy costs are small compared to the cost of the concentrate, it costs well over \$2000.00 per month in electricity to run the fans, and to remove the heat they generate from the tunnel.

Unfortunately, operating the freeze tunnel is more complicated than assumed in this analysis. The concentrate inlet temperature varies, the can size varies, and the rate of production varies. Therefore, one optimum operating point cannot be chosen. Although

a Nu of 90 and T_a of -25°F will adequately cool 12 ounce cans, it may not adequately cool a larger can unless the conveyor belt and production is slowed down. Some reserve capacity is needed. In general it would be desirable to maintain the lowest reasonable air temperature when the tunnel is operated at a higher capacity. If the product or cooling load changes, fans should be turned on and off as necessary to provide the desired exit temperature.

In the freeze tunnel observed, fans could not be secured selectively because all the fans operate in parallel with common inlet and outlet plenums. Some type of automatic damper system would be required to shut when the fan was secured to prevent reverse air flow through the idle fan. Assume a lower air temperature would allow 1 fan to be secured for half its normal operating time. During a 9 month season, almost \$1000.00 could potentially be saved in electricity costs for that fan. Savings this large could justify an inexpensive damper system.

4.8 RESULTS FOR FREEZE TUNNEL DESIGN IN GENERAL

Constructing a freeze tunnel is one of the largest initial expenses when building a food processing plant [1]. It is obvious that minimizing K will reduce the operating expenses of the tunnel. But the design must take into account trade offs between the initial investment capital and final operating expenses. However, many important trends that apply to freezing 12 ounce cans of citrus concentrate will have some relevance to any freeze tunnel where the needed useful refrigeration effect needed is large.

The lowest operating costs occur at the coldest air temperatures because the freezing times are shorter, and the tunnel's capacity is greater. On the other hand, for a given air temperature, the lowest operating costs occur for the lowest Nu , and consequently the longest freezing time. This means the freeze tunnel should be designed to provide an adequate freezing time, but no shorter than necessary. The fans should be chosen to provide this freezing time with the lowest reasonably producible air temperature. If the capacity varies, the fans should be operated selectively to maintain the lowest effective value of K .

EXTRA 100% BAG

CHAPTER 5
CONCLUSIONS

THESIS 10

5.1 LIMITATIONS OF STUDY

Use of the fan laws to relate the Nusselt number and characteristic air velocity to fan horse power limits the range of accurate predictions to operating conditions close to those of the observed tunnel. Predictions for operating conditions significantly different from the observed conditions are only rough approximations. Many of the operating conditions investigated in theory may not be achievable in application.

For example, a minimum fan horsepower may be required to produce any significant air flow through the evaporators and food product. This limitation on the minimum fan horsepower was not considered in this report.

The investigation assumed that characteristics of the refrigeration plant, and associated COP and temperatures, were for a two-stage ammonia vapor compression plant. The COP's used were rough approximations. Different COP's and air temperatures may be achievable with different types of equipment.

Also, the relationship between the Nusselt number, the air temperature, and the freezing time varies with the product cooled,

and the range of temperatures through which the product is cooled. Because of this, the graphs and numerical estimates may not be applicable to freeze tunnels cooling significantly different products.

5.2 SIGNIFICANT RESULTS

The major value of this investigation is the trend and the relationship between, the energy consumption, the Nusselt number, the air temperature, and the ratio of fan work divided by useful refrigeration effect. In review, the most economical energy consumption occurs, for large freeze tunnels, when the freezing times are no shorter than required, the air temperature is the lowest achievable value, and the ratio of fan work divided by useful refrigeration effect is the lowest achievable value.

Although some efficiency of the refrigeration unit is lost by producing a low air temperature, this trend is more than offset by the increased freeze tunnel capacity, and freeze tunnel coefficient of performance.

The significance of the ratio of fan work divided by the useful refrigeration effect, K , was also important. The energy expended to produce the desired cooling effect per unit of food product is determined predominantly by the value of K for the freeze tunnel. The minimum achievable values of K depend on the freeze tunnel design, the required refrigeration effect, and properties of the food product. The range of values for K measured for the observed freeze tunnel are reasonably accurate and could

be used to compare the effectiveness of the observed tunnel to another.

The equation for the freeze tunnel's coefficient of performance, equation (15),

$$COP_t = \frac{COP}{1 + (1+COP)K}$$

can be used by freeze tunnel operators and designers to estimate the freeze tunnel effectiveness. The heat content of the food product and the amount of food product in the tunnel would have to be determined. The freezing times can be estimated for a variety of products, and should be known by the tunnel operator. The horsepower of the fans is fixed, or determinable, so K may be calculated frequently without any other knowledge than that of the freeze tunnel design and the thermal properties of the food product. If the COP can be estimated, then COP_t can also be estimated.

5.3 POSSIBILITIES FOR FURTHER RESEARCH

It would be interesting to estimate and collect operating conditions for as wide a variety of freeze tunnels as available. One value of this would be to determine what minimum values of K may be achieved for specific food products. This information would be valuable in minimizing energy consumption in future designs or modifications to existing equipment.

Another valuable result of finding more operating points is that figures similar to those in this report could be generated with more accuracy, and potentially used as standards or guides for freeze tunnel design. Fan laws and other simple approximations

could be used to generate the portions of the graphs between the known operating points.

APPENDIX:

SAMPLE COMPUTER LISTING


```

$JOB
C CALCULATION OF AVERAGE TEMPERATURE OF A PACKED BED OF JUICE CONCENTRATES
C IN A FREEZE TUNNEL FOR VARIABLE THERMAL PROPERTIES AND A
C NINE ELEMENT MODEL
DIMENSION T (3,3), TP(3,3), V(3,3), H(2), K(3,3), S(3,3), HC(3,3)
DIMENSION C (3,3), K1 (3,3), K2(3,3)
REAL K, K1, K2, KI, LMTD
DO 210 N=1, 4
READ (5,11) H(1), H(2)
11 FORMAT (2F10.0)
READ (5,12) TI, TA1, TA2, TA3
12 FORMAT (4F10.0)
READ (5,13) HGT, RAD
13 FORMAT (2F10.0)
READ (5,14) U, TL, DELT
14 FORMAT (3F10.0)
C DEFINE AREAS
AEND = 3.1415926 * RAD ** 2
ACYL3 = 6.2831853 * RAD * HGT
ACYL2 = 0.8 * ACYL3
ACYL1 = 0.4 * ACYL3
C DEFINE VOLUMES
VTOT = HGT * AEND
V(1,0) = 0.04 * VTOT
V(1,2) = 0.12 * VTOT
V(1,3) = 0.09 * VTOT
V(2,1) = 2.0 * V(1,1)
V(2,2) = 2.0 * V(1,2)
V(2,3) = 2.0 * V(1,3)
V(3,1) = V(1,1)
V(3,2) = V(1,2)
V(3,3) = V(1,3)

```


C DEFINE INITIAL TEMPERATURE DISTRIBUTION AND THERMAL PROPERTIES

SI = 75.2
KI = 0.18
HCI = 0.73
D0 30 I = 1,3
D0 40 J = 1,3
S(I,J) = SI
K(I,J) = KI
HC(I,J) = HCI
C(I,J) = S(I,J) * HC(I,J) * V(I,J)
T(I,J) = TI

40 CONTINUE
30 CONTINUE

C DEFINE MISC TERMS

DELZ = HGT / 2.0
DELR = RAD / 2.5
TAVE = TI
TA = TAI
DI = 100.0
DT1 = DELT * 60.0 / DT
DT2 = DELT * 60.0
ER = 0.0

L = 1
M = 1

L0 = 0

C DEFINE RESISTANCES

C AXIAL CONDUCTION

AKEND = (0.75 * DELZ) / (AEND)
AK1Z = AKEND / 0.16
AK2Z = AKEND / 0.48
AK3Z = AKEND / 0.36

C RADIAL CONDUCTION

AK11R = (DELR * 6.0) / ACYL1
AK12R = (DELR * 3.0) / ACYL2


```

AK21R = 0.5 * AK11R
AK22R = 0.5 * AK12R
WRITE (6,90) H(1), TI, RAD, TL, H(2), TA, HGT, U, DT1, DT2
90 FORMAT ('1', 'VARIABLE THERMAL PROPERTIES FOR BRIX NO 44.8'// ' H(1)
1=', F5.2, ' BTU/HR-FT2-F', 4X, 'TI =', F6.1, ' F', 5X, 'RAD =', F7.4, 'FT',
25X, 'TL =', F6.1, ' FT'// ' H(2) =', F5.2, ' BTU/HR-FT2-F', 4X, 'TA =',
3F6.1, ' F', 5X, 'HGT =', F7.4, ' FT', 5X, ' U =', F6.1, 'FT/HR'//1X, F5.3,
4' MINUTE ITERATIONS AND DATA IS PRINTED EVERY ', F5.3, ' MINUTES',
5////)
WRITE (6,99)
99 FORMAT (1X, 5H TIME, 10H T(1,0), 10H T(2,1), 10H T(3,1),
110H T(1,2), 10H T(2,2), 10H T(3,2), 10H T(1,3), 10H T
2(2,3), 10H T(3,3), 10H TAVE, 10H TA3 //)
WRITE (6,100) LO, T, TAVE, TA3
100 FORMAT (I6, 11F10.1)
C COMPUTE NEW TEMPERATURE DISTRIBUTIONS
DELT = DELT / DT
DO 70L = 1, 100
C DEFINE FLOW DEPENDANT RESISTANCES
C END TO AMBIENT
RHEND = 1.0 / (H(M) * ΔEND)
RH11Z = RHEND / 0.16
RH12Z = RHEND / 0.48
RH13Z = RHEND / 0.36
C SIDES TO AMBIENT
RHSID = 1.0 / (H(M) * ACYL3)
RH13R = 4.0 * RHSID
RH23R = 2.0 * RHSID
DO 75 N = 1, 100
TP (1,1) = DELT/C(1,1)*(TA1/RH11Z+K(1,1))*(T(1,2)/AK11R+T(2,1)/AK1Z
1)+(1.-DELT/C(1,1))*(1./RH11Z+K(1,1))*(1./AK11R+1./AK1Z))*T(1,1)
TP(1,2) = DELT/C(1,2)*(TA1/RH12Z+K(1,2))*(T(1,1)/AK11R+T(1,3)/AK12R
1+T(2,2)/AK2Z)+(1.-DELT/C(1,2))*(1./RH12Z+K(1,2))*(1./AK11R+1./AK12R
2+1./AK2Z))*T(1,2)
TP(1,3) = DELT/C(1,3)*(TA1/RH13R+TA1/RH13Z+K(1,3))*(T(1,2)/AK12R+T(

```



```

12,3)/AK3Z))+(1.-DELT/C(1,3)*(1./RH13Z*1./RH13R+K(1,3))*(1./AK12R+1.
2/AK3Z)))*T(1,3)
TP(2,1) = DELT/C(2,1)*K(2,1)*(T(1,1)/AK1Z+T(2,2)/AK21R+T(3,1)/AK1Z
1)+1.-DELT/C(2,1)*K(2,1)*(2./AK1Z+1./AK21R))*T(2,1)
TP(2,2) = DELT/C(2,2)*K(2,2)*(T(2,1)/AK21R+T(1,2)/AK2Z*T(2,3)/AK22
1R+T(3,2)/AK2Z)+(1.-DELT/C(2,2)*K(2,2)*(1./AK21R+2./AK2Z+1./AK22R))
2)*T(2,2)
TP(2,3) = DELT/C(2,3)*(TA2/RH23R+K(2,3)*(T(2,2)/AK22R+T(1,3)/AK3Z+
1T(3,3)/AK3Z))+(1.-DELT/C(2,3)*(1./RH23R+K(2,3))*(1./AK22R+1./AK3Z))
2)*T(2,3)
TP(3,1) = DELT/C(3,1)*(TA3/(RH11Z+442.15)+K(3,1)*(T(3,2)/AK11R+
1T(2,1)/AK1Z))+(1.-DELT/C(3,1)*(1./RH11Z+442.15)+K(3,1)*(1./AK11R+
21./AK1Z))*T(3,1)
TP(3,2) = DELT/C(3,2)*(TA3/(RH12Z+147.38)+K(3,2)*T(3,1)/AK11R+
1T(3,3)/AK12R+T(2,3)/AK2Z))+(1.-DELT/C(3,2)*(1./RH12Z+147.38)+
2K(3,2)*(1./AK11R+1./AK12R+1./AK2Z))*T(3,2)
TP(3,3) = DELT/C(3,3)*(TA3/RH13R+TA3/(RH13Z+196.51)+K(3,3)*T(3,2)
1/AK12R+T(2,3)/AK3Z))+(1.-DELT/C(3,3)*(1./RH13R+1./RH13Z+196.51)+
2K(3,3)*(1./AK12R+1./AK3Z))*T(3,3)

```

C REDEFINE TEMPERATURE DEPENDENT THERMAL PROPERTIES AND TEMPERATURES

```

D0 50 I = 1,3
D0 60 J = 1,3
T(I,J) = TP (I,J)
IF ( T(I,J) .GE. 15.5) GO TO 51
IF ( T(I,J) .LE. -19.0) GO TO 52
K1(I,J) = 0.00074*T(I,J)**3 - 0.0040*T(I,J)**2 + 0.0032*
1T(I,J) + 0.35
K2(I,J) = 0.00013*T(I,J)**3 + 0.0042(T(I,J)**2 + 0.017*T(I,J)
1+0.35
IF ( T(I,J) .LT. 0.0 ) K(I,J) = K2(I,J)
IF ( T(I,J) .GE. 0.0 ) K(I,J) = K1(I,J)
S(I,J) = 0.000019*T(I,J)**3 + 0.0023*T(I,J)**2 + 0.10*T(I,J)
1+73.00
HC(I,J) = 0.0046*T(I,J)**2 + 0.14*T(I,J) +2.0
IF ( T(I,J) .LT. -19.0) HC(I,J) = 1.00

```



```

C(I,J) = S(I,J) * HC(I,J) * V(I,J)
GO TO 60
CONTINUE
51 K(I,J) = KI
HC(I,J) = HCI
S(I,J) = SI
C(I,J) = S(I,J) * HC(I,J) * V(I,J)
GO TO 60
CONTINUE
52 K(I,J) = 0.65
HC(I,J) = 1.00
S(I,J) = 71.77
C(I,J) = S(I,J) * HC(I,J) * V(I,J)
60 CONTINUE
50 CONTINUE
C CALCULATE RETURN AIR TEMPERATURE
ATOT = 2.0*AEEND + ACYL3
TS = (T(2,3)*0.5*ACYL3+(T(1,1)+T(3,0))*0.16*AEEND+(T(1,2)+T(3,2))*
10.48*AEEND+(T(1,3)+T(3,3))*(0.36(AEEND+0.25*ACYL3)))/ATOT
LMTD = (TA3 - TA1)/ALOG((TS - TA1)/(TS - TA3))
TA3 = TA1 + 0.24 *LMTD
TA2 = (TA1 + TA3)/2.0
75 CONTINUE
C CALCULATE AVERAGE TEMPERATURE
TAVE = 0.0
DO 80 I = 1,3
DO 85 J = 1,3
TAVE = TAVE + V(I,J)*( T(I,J) /VTOT
85 CONTINUE
80 CONTINUE
WRITE (6,100) L, T, TAVE, TA3
IF (TAVE .LE. -5.0) GO TO 210
70 CONTINUE
210 CONTINUE
STOP
END

```


REFERENCES CITED

- ¹ASHRAE Handbook and Product Directory 1978 Applications. New York : American Society of Heating, Refrigeration, and Air-Conditioning Engineers, 1978, pp. 25.1-25.8.
- ²Porter, Wendell A., and Bishop, P.J. "Analysis of Energy Use and Recommendations for Potential Savings at a Citrus Concentrate Plant in Florida." Orlando: University of Central Florida, Engineering and Industrial Experiment Station Report, August 1979.
- ³ASHRAE Handbook and Product Directory 1977 Fundamentals. New York: American Society of Heating, Refrigeration, and Air Conditioning Engineers, 1977, p. 1.2.
- ⁴Ibid., pp. 27.1-27.5.
- ⁵Ibid., p. 22.6.
- ⁶Chen, C. S. "Specific Sheet of Citrus Juice and Concentrate." Proceedings of the Florida State Horticultural Society 92 (June 1979): 154-6.
- ⁷Saitoh, T. "Numerical Method for Multidimensional Freezing Problems in Arbitrary Domains." ASME Journal of Heat Transfer 100 (May 1978): 294-9.
- ⁸Landau, H.G. "Heat Conduction in a Melting Solid." Quarterly Journal of Applied Mathematics 81 (April 1950): 81-94.
- ⁹Keller, George J., and Ballard, John H. "Predicting Temperature Changes in Frozen Liquids." Industrial and Engineering Chemistry 48 (February 1956): 188-96.
- ¹⁰Whitaker, Stephen, "Forced Convection Heat Transfer Correlations for Flow in Pipes, Past Flat Plates, Single Cylinders, Single Spheres, and for Flow in Packed Beds and Tube Bundles." American Institute of Chemical Engineering Journal 18 (March 1972): 361-71.
- ¹¹Holman, J.P. Heat Transfer. 4th ed. New York: McGraw-Hill, 1976 , pp. 123-38.
- ¹²Roberson, John A. and Crowe, Clayton T. Engineering Fluid Mechanics. Boston: Houghton Mifflin Company, 1975, pp. 418-20.
- ¹³ASHRAE Handbook and Product Directory 1975 Equipment. 2nd ed. Menasha, WI: George Banta, 1978, pp. 3.1-3.12.